A MAJOR PROJECT REPORT

on

EXPERIMENTAL STUDY OF MECHANICAL AND TRIBOLOGICAL PROPERTIES OF AA6063 AND MARBLE DUST COMPOSITES FABRICATED BY FSP

Submitted in partial fulfillment for the award of the degree

of

MASTER OF TECHNOLOGY

in

PRODUCTION ENGINEERING

by

VIKAS

(2K17/PIE/20)

UNDER THE GUIDANCE

OF

Dr. R. C. SINGH

DEPARTMENT OF MECHANICAL, PRODUCTION AND INDUSTRIAL ENGINEERING

DELHI TECHNOLOGICAL UNIVERSITY

Bawana Road, Delhi-110042

JUNE-2019

CANDIDATE'S DECLARATION

I, **Vikas**, 2K17/PIE/20 hereby declare that the major project Dissertation titled "**EXPERIMENTAL STUDY OF MECHANICAL AND TRIBOLOGICAL PROPERTIES OF AA6063 AND MARBLE DUST COMPOSITES FABRICATED BY FSP"** submitted to the department of MECHANICAL, PRODUCTION & INDUSTRIAL ENGINEERING, Delhi Technological university, Delhi in partial fulfillment of the requirement for the award of the **Master of Technology**, in **Production Engineering** was original and not copied from any source without proper citation. This was further to declare that the work embodied in this report has not previously formed the basis for the award of any Degree, Diploma Associateship, Fellowship or other similar title or recognition.

Place: Delhi **Vikas**

Date: (2K17/PIE/20)

CERTIFICATE

I hereby certify that the major project entitled **"EXPERIMENTAL STUDY OF MECHANICAL AND TRIBOLOGICAL PROPERTIES OF AA6063 AND MARBLE DUST COMPOSITES FABRICATED BY FSP",** in partial fulfillment of the requirements for the award of the Degree of **Master of Technology** in **Production Engineering** and submitted to the Department of Mechanical, Production and Industrial Engineering of Delhi Technological University has been an authentic record work of **Mr. Vikas (2K17/PIE/20)** carried out under my supervision.

It is to further certify that the matter embodied in this report has not been submitted to any other university or institution by him for the award of any other Degree/Certificate and the declaration made by him is correct to the best of my knowledge and belief.

Dr. R. C Singh
Professor
Department of Mechanical Engineering
Delhi Technological University

Place:

Date:

ACKNOWLEDGMENTS

I would like to express my special thanks of gratitude to Dr. R. C Singh for their guidance, unwavering support and encouragement. This project work could not have attained its present form, both in content and presentation, without his active interest, direction and guidance. His personal care has been the source of great inspiration. He has devoted his invaluable time and took personal care in motivating me wherever I was disheartened.

I would also like to thank Prof. Vipin, HOD (Mechanical Engineering Department), Prof. Ranganath M. Singari, Prof. Rajiv Chaudhary, Dr. N. Yuvraj, Prof. Quasim Murtaja, Prof. Vijay Gautam, Mr. Sumit Chaudhary and Dr. Bharti for their support and guidance, although they had a very busy schedule in managing the corporate and academic affairs.

I am thankful to the technical staff of Delhi Technological University, Mr. Manjeet, Mr Pradeep, Mr. Sunil, Mr. Lalan, Mr. Sandeep, Mr. Tek Chand for their support.

My deep and sincere gratitude to my family for their continuous and unparalleled love, help and support. I am grateful to my sister, mausee for always being there for me as a friend and always with me in every situation. I am forever indebted to my parents for giving me the opportunities and experiences that have made me who I am. They selflessly encouraged me to explore new directions in life and seek my own destiny. This journey would not have been possible if not for them, and I dedicate this milestone to them. I cannot forget to take the name of my cousins for helping me to manage the time and managing my journey to complete the project work.

I also want to thank all those who are directly or indirectly supports me for my project.

Vikas

(2K17/PIE/20)

Table of Content

LIST OF TABLES

LIST OF FIGURES

ABBREVIATIONS

F.S.P	Friction Stir Processing
FSW	Friction Stir Welding
M.S	Microstructure
S.C	Surface Composites
M.P	Mechanical Properties
U.T.S	Ultimate tensile strength
Y.S	Yield Strength
F.A	Fly Ash
B.M	Base Material
POD	Pin on Disc
Sample-1	Base material AA6063
Sample-2	AA6063/Marble Dust at room temperature
Sample-3	AA6063/Marble Dust pre-heat at 100^{o}C
Sample-4	AA6063/Marble Dust pre-heat at 200^{o}C

ABSTRACT

The aluminium composites nowadays are replacing conventional materials from many industrial, home, architecture, aerospace, automobile industries, etc. as the vast use of MMC over conventional material, research work in this field increases. The was to analyze the effect of Marble Dust (M.D) on the grain structure, mechanical properties, and tribological properties. X-Ray Diffraction test is done for the characterization of the prepared samples. It reveals the composition of elements present in the MMC's. Field scanning electron microscope also done to check the wear track and type of wear of a prepared composite. AA6063/M.D composite fabricated using F.S.P technique. Four samples were prepared for analysis, sample-1 AA6063 base material, sample-2 AA6063/M.D processed at room temperature. Sample-3 AA6063/M.D processed at pre-heat 100^{o}C temperature and sample-4 AA6063/M.D processed at pre-heat 200^{o}C temperature.

The sample-4 gives maximum Ultimate Tensile Strength of 202 MPa. The vicker's hardness of sample-4 is 29% more than then the base material. Sample-4 exhibits 15% increment in the micro-hardness as compared with sample-1. The microhardness of the sample-1 67.29 MPa, Sample-2 57.63, Sample-3 59.75 and sample-4 77.396 Hv.

The FESEM images revels the type of wear and defects present over the surface of the material after wear. The microstructure shows finer grain structure and good bonding b/t marble dust and AA6063. The composite material showed better tribological properties as compared with AA6063.

The Taguchi analysis revels that among all the input parameters speed has maximum impact on Coefficient of Friction (COF) and temperature had maximum impact on specific wear rate (SWR) for base material. In case of composite material sliding speed had minimum impact on COF and load had least impact on SWR.

Keywords:- F.S.P, FSW, XRD,FESEM, marble dust, MMC's

CHAPTER 1

INTRODUCTION

At first, Friction Stir Processing (F.S.P) was used for microstructural refinement of aluminum and magnesium mixes. F.S.P progression has encouraged prompted the productive treatment of composites of titanium, copper, and steel. F.S.P has in like manner displayed its viability in homogenizing powder metallurgy handled with aluminum mixes, microstructural alteration of metal system composites. F.S.P satisfactorily eliminates throwing abandon, isolates or disintegrates second stage particles and brief the broad improvement in properties [14].

F.S.P has certain advantages to contrast with other metal work strategies. To begin with, F.S.P was a prompt solid-state strategy that attends microstructural change, densification, and homogeneity in the meantime. Second, by modifying the design of the experiment, F.S.P parameters, and dynamic cooling/warming the M.S and mechanical properties of the zone can be conclusively regulated. Third, the profundity of the prepared zone can be alternatively constrained by modifying the length of the tooltip. Fourth, having a wide limit F.S.P was a versatile strategy with regards to the manufacturing, taking care of, an amalgamation of materials. Fifth, F.S.P was a green and essentialness successful strategy without frightful gas, radiation, and commotion since the warmth contribution in the midst of F.S.P begins from grinding and plastic twisting. sixth, F.S.P does not adjust the shape and size of the prepared examples [13].

Created the Sic/Al S.C by F.S.P, and demonstrated that SiC particles were well distributed in the Al matrix, and great holding with the Al grid was produced. There were various customary strategies for manufacturing S.C, for example, powder metallurgy, laser soften treatment, plasma showering, mix throwing and so forth yet these methods lead to the crumbling of composite properties because of interfacial reaction among reinforcement and the metal matrix [32].

F.S.P/FSW was a Green Technology because it doesn’t pollute the environment while working [13]. These strategies include the material change from solid to liquid or vapor state during the procedure when contrasted with solid state handling system. In addition,

exact control of processing parameters was required to get desired M.S in the surface layer after solidification. F.S.P was one of the solid-state processing technique which has demonstrated its potential in the manufacture of all variations of S.C with practically no interfacial response with the reinforcement. The potential utilization of S.C can be found in car, aviation, marine and power age businesses. In spite of impressive interests in the F.S.P innovation in the past decade, the essential physical comprehension of the procedure was deficient. Some significant perspectives, including material flow, tool geometry configuration, wear of F.S.P tool, microstructural, welding of divergent alloys and metals [33].

1.1. Material selection

1.1.1. Aluminium

a. Aluminium and its alloys

Aluminium has a very wide classification of its alloys, these were the base of the aeronautical industry. It also utilized to help with cooking and packing. It helps in the production of high-grade steels and it was additionally used for the base of flexible paint. Pure aluminum was delicate, malleable, and corrosion resistant in nature and has a high electrical conductivity.

Aluminium was generally utilized for foil and conductor links. Including other alloying components increases the quality of aluminum composite for different applications. Aluminum was light and appealing metal showing a high level of corrosion resistance in the corrosive surrounding [13]. It was likewise delicate, hard, simple to weld, hard to weld, and a large group of other apparently clashing qualities. The properties of a specific aluminum item depend upon the compound picked. The term aluminum alludes to a family of alloys. Information of these alloys was the way to the use of aluminum properly. On an international basis, the major step was taken towards alignment of Aluminium and its alloy compositions, for alloy composition designation most nations have agreed to adopt the 4-digit characterization. This system was controlled by the Aluminum Association (AA), Washington USA, who arrange the ″Registration record of International Alloy Designations and Chemical Composition Limits for Wrought Aluminum Alloys″. The European reference for the alloys will be related to the introduction EN and AW which showed European Normative Aluminum Wrought Alloys. In every other regard, the alloy

numbers and organization limits were indistinguishable to those enlisted by the Aluminum Association. The first of the four digits in the assignment shows the alloy group regarding the major alloying components [40]. The family of aluminum compounds which were promptly accessible worldwide.

b. Designation of Aluminium

The aluminium alloy was characterized on four digits(xxxx).

The first digit (Xxxx): - It defines the principal alloying element, this alloying element was added in aluminium. Some aluminum alloy series were described as 1000, 2000, 3000, up to 8000 series**.**

The second digit (xXxx): - It was basically 0 if there was no modification made in the aluminium series. If it was not 0, it indicates a modification in that specific alloy,

Third & Fourth digits (xxXX): - were the arbitrary numbers given to the specific alloy in the series.

6XXX series: - As 6xxx has good mechanical properties such as strength, formability and corrosion resistance, they were regarded as the most promising applicants for the automotive industry. This series alloy also was known as Al-Mg-Si-Cu alloys [41]. During pain-back cycle the strengthening agent(Mg_2Si) was formed from Mg and Si elements [35]. An excess of silicon in the T4 state has the impact of growing formability [42,43], and the distribution of reinforcement stages during under peak artificial aging was also refined. The refinement of precipitate M.S has described a result of a reduction in solubility of Mg_2Si with Si content above the ' balanced ' proportion [44]. As the composition of Si increased, this composition has adverse effects on heat stability [45,46] and improved sensitivity to intercrystalline corrosion due to the silicon grain boundary segregation [47,48]. Silicon improves the comparative strength of the harmful As-cast β-AlFeSi particle, however, adequate alloy and heat treatment can overcome this.

1.1.1.1. AL6063: -

It was an aluminium alloy, with the major alloying element as magnesium and silicon. The chemical composition of aluminium used in this study was shown in Table 1. These results were verified by chemical spectroscopy. The mechanical properties of the aluminium 6063 were shown in Table 2.

Chemical Composition:

Table 1 Al6063 Chemical Composition

Elements	Si	Fe	Mg	Mn	Ti	Zn	Ni	Cr	V	Sr	Al
Mean	0.64	0.2732	0.6941	0.1074	0.0736	0.0693	0.039	0.0345	0.035	0.0005	98.01

Mechanical Properties:

Table 2 Mechanical Properties of Al6063

AA6063	
Physical Properties	
Young's Modulus	68.3 GPa
Tensile Strength	145-185 MPa
Elongation	18-33%
Powasson's Ratio	0.3
Thermal Properties	
Melting Temperature (Tm)	615^{o}C
Thermal Conductivity(k)	201-218 W/m*K
Coefficient of Liner thermal expansion(α)	$3.34\times10^{-5}k^{-1}$
Specific heat Capacity(c)	900J/KgK

Advantages of Aluminium alloy:

1. It has good resistance to general corrosion and provides resistance to the stress cracking corrosion.
2. It has a very good surface finish and good extrudability.
3. It offers an excellent response for anodizing.

Applications of Aluminium alloy:

- Products for architecture and construction
- Frames for doors and windows
- Electrical and conduit elements

- Equipment and Railings
- Irrigation pipes and tubes
- Heat-sinks

1.1.2. Marble Dust

Factually, marbles were the natural stones having calcareous ($CaCO_3$) and dolomite $CaMg(CO_3)$ major elements in marble dust. The other main elements in marble dust were shown in Table 4. The marble dust which was used as reinforcement, shown in Figure 1. There were two types of waste obtained while cutting and polishing of marble. First waste was during the cutting and polishing of the marble dust was called marble waste slurry (MWS) and the second waste was the broken pieces of marble. The total quantity of waste obtained while processing the blocks and slabs of marbles varies with the machining process was between 30% and 50% of the volume of all processed blocks. These wastes affect both nature and the economy and have harmful effects. The solid waste of marbles was stored in the huge factory warehouses. The marble slurry was refined as much as possible from the water through the treatment unit and the marble waste sludge was obtained. This amount of waste was too large for marble companies to be able to store. For this reason, with controlled or uncontrolled access, these marble waste were dumped into nature. Because of this, the waste causes considerable pollution of the environment. So the use of the marble dust decreases pollution and increases the economic benefits.

Figure 1 Marble Dust

The composition of Marble Dust:

Table 3 Marble Dust composition [48]

Components	**Wt%**
CaO	42.45
MgO	1.52
SiO_2	26.35
Al_2O_3	.520
Fe_2O_3	9.40

1.1.3. Tool Materials

FSW tool specifications and material properties were very critical to select and designing of the tooltip. The tool material was basically depending on the application of tool and type of work-piece. The following properties for F.S.P tool were important for manufacturing and designing of it.

(i) At high temperature, higher compressive yield strength than anticipated forge forces on the instrument.

(ii) It should have good strength, dimensional stability and crude resistance.

(iii) Performance of a tool should be good at repeatedly cooling and heating cycles.

(iv) It should not react with the work-piece material.

(v) The toughness of a tool material should be high to reswast the damage during dwelling and plunging.

(vi) tool material should have a low thermal coefficient of expansion.

(vii) Good machinability.

(viii) The cheaper or affordable price of the material.

1.2. Tool Shape

The tool was consisting of prob/tip, shoulder to generate frictional heat and apply the required downward force to consolidate and maintain the soften metal underneath of shoulder surface. Generally, the outer surface of shoulder consists of conical or cylindrical in shape. The diameter of the shoulder and tip were in a ratio of 3:1. Type of shoulders was classified into three types as shown in Figure 2, but the most common and straight forward

design was the flat shoulder end surface. This shoulder can't hold entrap the material under the shoulder surface and the unwanted material flashed out. As it may be, an inwardly curved shoulder end surface was designed to restrict material expulsion from the shoulder edges [33].

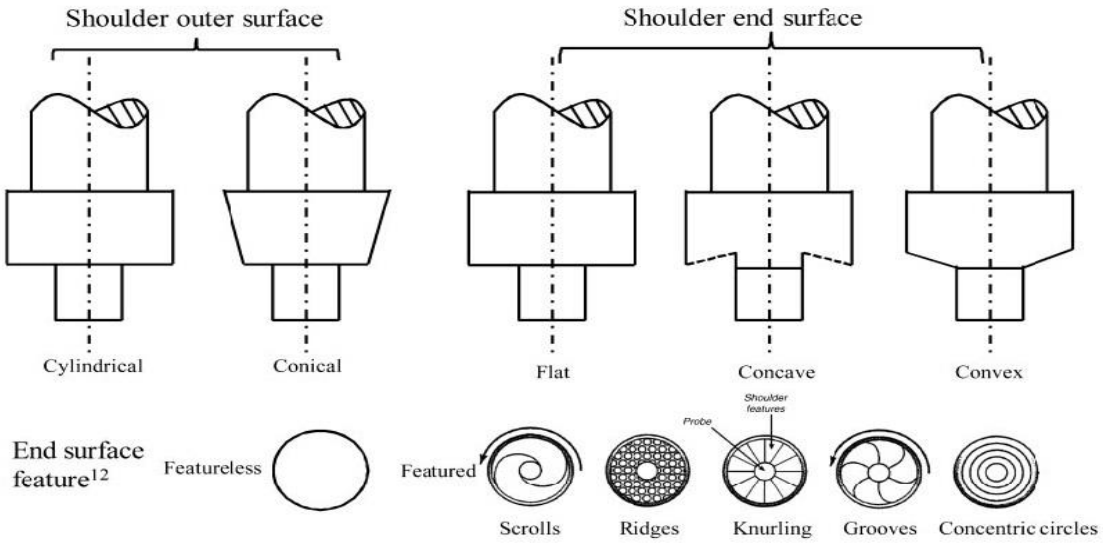

Figure 2 Type of Shoulder [36

A convex curve profile was another practical end condition of the shoulder [35]. By convex shoulder profile the joining of workpieces via friction stir welding, the main advantage was that contact with the workpiece can be made anywhere down the surface. Variety in level or thickness between the two attributable edges in this way. On the other side, the inability to prevent material removal from the pin leads to an unreliable weld using a convex shoulder profile [37].

The Tool Pin was mainly responsible for distributing the contacting surface of work-piece, cut the metal in face of the tool and move the plasticized metal behind the tool. The depth of processed zone and maximum traverse speed were controlled by the pin geometry. Figure 3 shows the different type of tooltip profile for processing. Various forms and characteristics, including threads, apartments or flutes, can be regarded on the exterior surface of the pin. Threadless pins were better options for processing high strength or highly abrasive alloys as these characteristics can be readily worn away [38]. The flat surface characteristics of the pin, the local plasticized were a and the rigorous (turbulent)

flow of the plasticized material can change the motion of metal material around the pin [39].

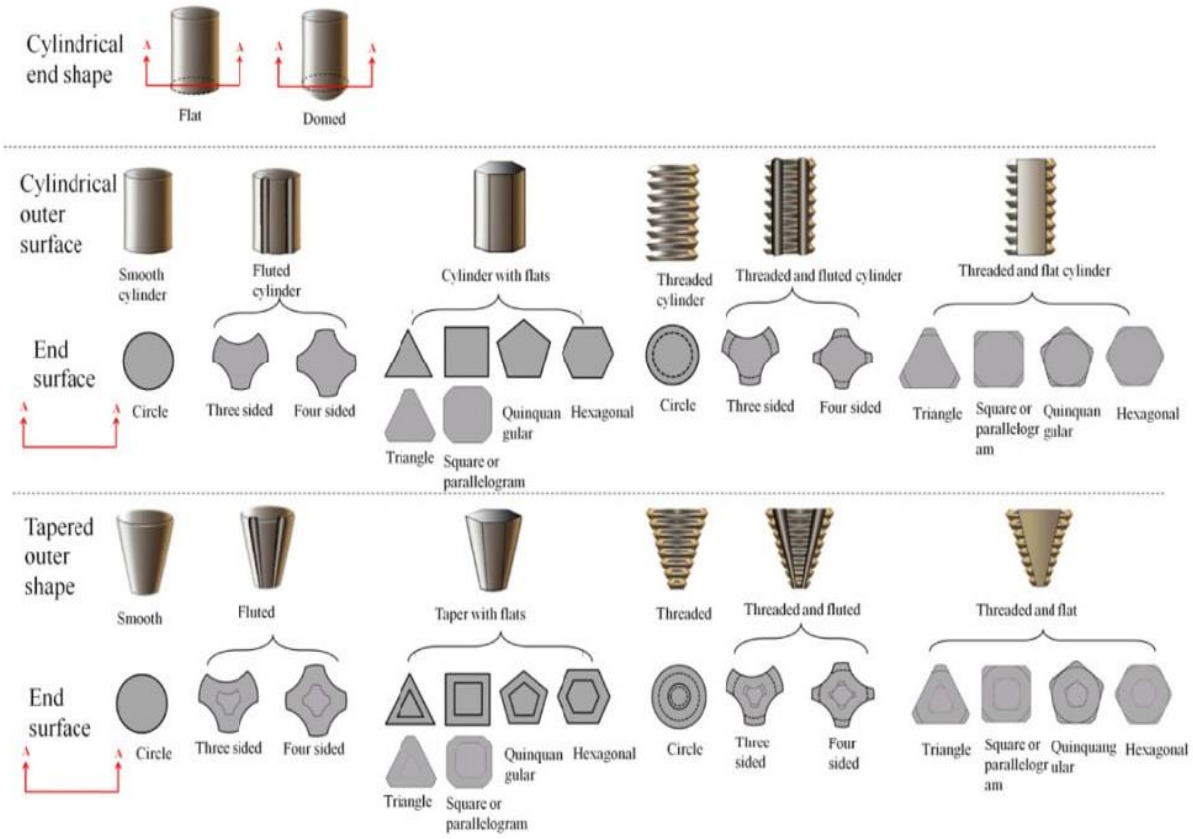

Figure 3 Tool Shapes[37]

1.3. Techniques of Fabrication

1.3.1. Friction Stir Processing

It enables the mechanical processing of a particular location on the structural surface and the improvement of specific properties to some significant depth (> 25 mm). The enhancement in properties was carried out on the FSW principal. The FSW technology was improving for F.S.P process. FSW was a process of joining metals which were hard to fuse or very difficult to weld by other processes. F.S.P was a process which was not used for welding, it was used to improve the properties of surface and improvement in the M.S. A cylindrical F.S.P tool with the probe was designed and it was rotated and plunged on the sheet or plate. By the rotation of the tool frictional heat was generated, this heat softens the

metal and by this property of metal changes. The penetration depth was controlled by the shoulder.

Locally, by F.S.P the casting defects were eliminated and it refines M.S. This process also improves mechanical properties like strength, ductility, fatigue resistance, formability, corrosion resistance, etc. In order to impart superplasticity, F.S.P has the ability to produce M.S with finer grain size throughout the thickness.

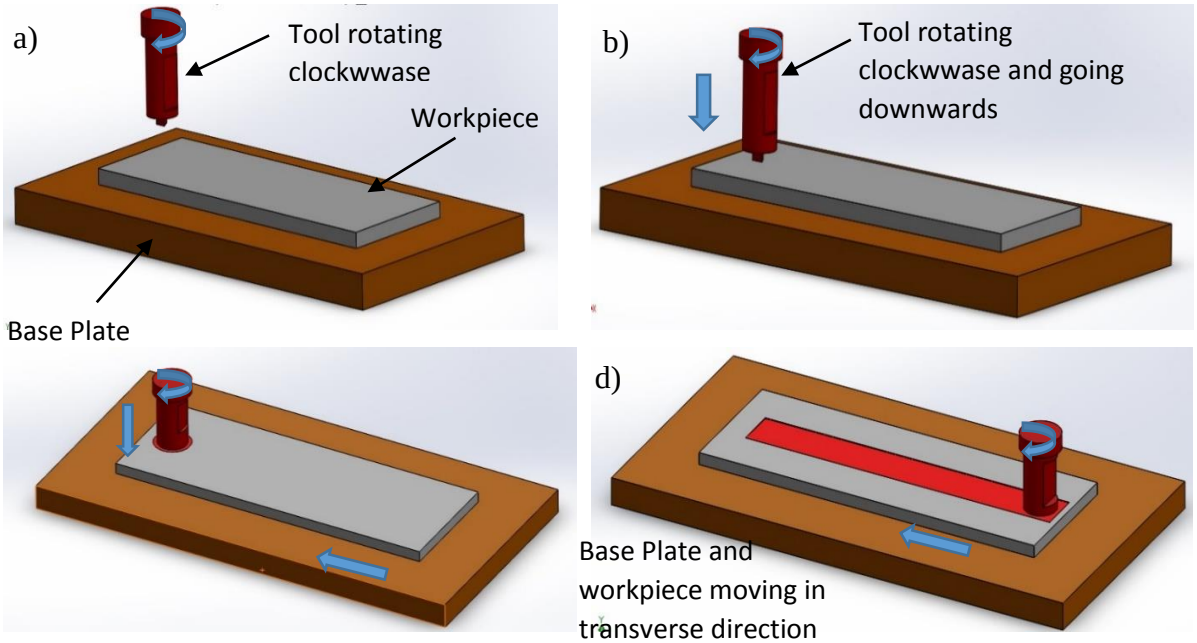

a) Rotating tool before plate contact.
b) Tool pin contacts the plate and produces heat from friction.
c) The shoulder contacts theW/P, penetration and frictional heat increases.
d) The plate moves towards the rotating tool, producing a fully recrystallized fine grain.

Figure 4 Procedure of F.S.P

Frictional heating and severe deformation lead throughout the tool's flow of plasticized material and consolidation in the tool's wake. This technique provides gradual changes in M.S. F.S.P zones can generate depths of 0.5 to 50 mm.

The basic processes of F.S.P contain as shown in Figure 4 has the tool that allowed to rotate and the tool brings near the workpioece. The rotating tool pin touch the workpiece surface, the downward motion of the tool was stopped and it allowed to rotate on the surface until

the temperature of the w/p higher enough. The shoulder offers a forging force that contains metal's upward flow triggered by the tool's pin. As shoulder touches the w/p surface, the tool and the w/p moved relative to each other. The processed area cools and leads to the formation of a recrystallized, fine grain M.S. without defects. Essentially, F.S.P was a local method of working with thermomechanical metals that changes local characteristics and structure without influencing other characteristics.

1.3.2. Powder Metallurgy

Powder metallurgy (P/M) was a unique approach to the manufacture of metal components that derives its meaning from several separate characteristics. The capacity to produce complicated components within tolerance limits was a main financial advantage. However, this low-cost, high-volume manufacturing technique imposes very specific quality assurance criteria. Three primary manufacturing steps were categorized by the Powder Metallurgy: powder mixing, green-state compaction, and sintering. It was the compaction method that provides the greatest pay-off for quality control through non-destructive evaluation (NDE) methods. The issue of forming defects in green components became more common during compaction and ejection as parts producers started using greater compaction pressures to obtain high-density and high-performance P/M components. It has been shown that the physical characteristics of P / M components were always enhanced by raising the density, especially the strength of fatigue.

1.3.3. Ultrasonic Probe Assisted Stir Casting

In this technique, the stir casting method was combined with ultrasonic probe processing. This process was named ultrasonic probe assisted stir casting method. This system works with Ultrasonic waves which have a recurrence of 18 to 20 kHz. At the point when these waves engender through the fluid medium, substituting pressure and enlargement cycles were delivered. The high-intensity ultrasonic waves at the end of rotating pressure and widening cycles influence the miniaturized scale rises to develop in the fluid. When they accomplish a volume at which they can never again assimilate enough vitality, they implode viciously. This was known as cavitation. Amid implosion, high temperatures and weights were come to inside these air pockets. Toward the finish of the cavitation cycle; crumple of small scale bubbles produces transient miniaturized scale problem areas that can achieve high temperatures and weights. Implosive effect of

cavitation was sufficiently able to break bunches of nanoparticles to scatter them consistently in the metal grid. The procedure joined the benefits of ultrasonic test and in addition mix throwing the process. The joined procedure will enhance the consistency in a scattering of nanoparticles because of ultrasonic cavitation impact and keep away from the settlement of nanoparticles in the metal grid because of persistent blending with the stirrer. This will deliver MMNCs which improved mechanical properties.

CHAPTER-2

LITERATURE REVIEW

This survey was done to recognize the techniques for the fabrication of metal matrix composite for various materials. In this section the study the main emphasis was to study the mechanical and tribological performance of MMC of AA.

Kenneth Kanayo Alaneme et al. (2018) [1] manufactured Al-Mg-Si alloy from Two-step stir casting method with groundnut shell ash and Sic to examine Microstructural and Mechanical properties. From this experiment, the author showed that tensile strength and fracture toughness of the composite increased but hardness and UTS decreased.

Kenneth Kanayo Alaneme et al. (2018) [2] used rice husk ash and Sic as reinforcement, aluminium alloy was used to form a composite by the double stir casting process. The author did this experiment to check the effect of corrosion on the composite. The author concluded that corrosion resistance increases as the percentage of RHM increased.

Govindharajan.B et al. (2015) [3] fabricated the composite Aluminium 6061 with FA, glass fiber with the help of stir casting method. The author studied the effect on mechanical properties and compared the results with the base material. The comparison was made between 4 samples of different composition of fly ash and glass fiber. The results show that the U.T.S, Y.S, compressive strength, % elongation and hardness of specimen increase as the content of fly ash increases.

M. Balakrwashnan et al. (2019) [4] used AA6061/Al3Zr AMCs (Aluminium matrix composite) to compare the results before and after fabrication of composite. The author found that casting defects such as porosity was eliminated by F.S.P and the finer, homogeneous distribution of grains was observed. The density, tensile strength and ductility of the composite increased.

M. Balakrwashnan et al. (2019) [5] used AA6061/Al3Fe AMC to enhance the properties of the composite. The author took the finer iron powder to Aluminium and F.S.P was done. Finer and homogenous distribution of grains was observed. By using F.S.P the author

observed casting defect such as porosity was eliminated. The UTS and ductility of the material improved.

Praveen Kumar Bannaravuri (2018) [6] compare the effect on density, tensile, hardness, impact strength, tribology, and M.S by fabrication of Al-4.5%Cu matrix alloy bamboo leaf ash by S.C technique. The author discovered from this experiment that the BLA spread evenly throughout the matrix. Density reduces as the percentage wt of BLA rises, the strength of tensile and hardness increases, the rate of wear decreases as the percentage wt of BLA rises.

Bharathi.V et al. (2017) [7] studied the effect on hardness, M.S, and density of reinforced pure aluminium with fly ash by stir-squeeze cast method. By this experiment, the author saw that as wt% of FA increases with load and speed lead to an increase in wear rate. As reinforcement increases hardness increases and density decreases.

Amba Chaithanyasai et al. (2014) [8] saw the effect on the density and hardness by the fabrication of Aluminum 6061 with eggshell by the powder metallurgy method. The author studied that the eggshell properly mixed in the matrix and good bounding between eggshell and Al powder. As wt% of eggshell increased the hardness of composite also increased.

Devaraju A et al. (2018) [9] studied the effect on the flexural test, impact test, and hardness test fabricated by epoxy and hardener technique with natural coconut fiber, epoxy, and hardener. The author reported that the load carrying capability increases, Impact, and hardness also increased.

Wasaac Dinaharan et al. (2018) [10] The impact of strengthened aluminum alloy AA6061, magnesium alloy AZ31, and copper with fly ash fabricated by F.S.P on microhardness and micro-structure was studied. The author discovered that, regardless of the type of metallic matrix, the micrographs revealed a homogeneous distribution of FA particles. The grains of the composites were widely refined due to the dynamic recrystallization and pinning impact of FA particles. The inclusion of FA particles enhanced all composites ' microhardness. F.S.P was an appropriate method for producing MMCs strengthened by FA irrespective of the type of matrix material used.

Dinaharan et al. (2019) [11] studied the effect on UTS and M.S by F.S.P on AA6061/Al_2Cu. The author noted that F.S.P broke down big Al_2Cu particles into fine particles because the tool's severe plastic strain and mechanical effect, this technique eliminated the typical casting defects owing to adequate plasticization and consolidation, and enhanced the tensile strength and ductility of cast composites owing to desirable microstructural modifications.

Wasaac Dinaharan et al. (2017) [12] fabricated the composite aluminum alloy AA6061 with by F.S.P and seen the effect on M.S, and tensile strength. The author saw the homogeneous distribution of RHA particles in the composite. Due to this pinning action, the grains were refined and RHA particles fragmented during F.S.P and the tensile strength was an improvement.

M. S Ranganath et al. (2014) [13] the author investigates the effect on properties of the material by the parameters affecting the F.S.P process. The parameter investigated such as the rotational speed of the tool, transverse feed rate, width and depth of the groove, axial load. By this investigation, they found that higher the RPM of tool and lower the processing speed or feed rate of the table gives an excellent distribution of material particles and the composite area also increases due to higher frictional heat. The author also found that lower the feed rate finer the grains size and use of triangular tool gives the better distribution of particles because the flow of material was more and area of the composite was more as compared with other tools.

M. S Ranganath et al. (2015) [14] seen the effect of multi-pass F.S.P (MF.S.P) on the 99.99% of copper with Carbon Nanotubes to improve the properties of composite material. The author studied that the fabrication was possible with carbon Nanotube with copper. As the amount of passes increased, the U.T.S get increased, and the Brinell hardness also improved due to the compact micro-structure.

J. Allwyn Kingsly Gladstone et al. (2017) [15] fabricated AA6061 with rice husk ash by composting to see the results on Wear rate, M.S. The author compared the outcomes and as grain refinement rises with enhanced RHA particle content. RHA particles enhanced composite wear property and increased hardness but as the load increased the wear rate also increases compared to the base metal.

Ch.Hima Gireesh et al. (2018) [16] studied the effect on density measurement, mechanical properties, tribological properties, and M.S of reinforced pure aluminium with fly ash and aloe vera by S.C method. The author demonstrates that composite strength improves in hardness, tensile strength. The UTS increases with fly ash and aloe vera was 31.44% and 55.62%. The density of pure aluminium was 2.70, AMC-FA-2.60 and AMC-AV-2.21, hardness and impact strength was pure aluminium<AMC-FA<AMC-AV.

Mohammed Imran et al. (2016) [17] Studied the impact of reinforced Aluminum-7075 hardness, Y.S and mechanical characteristics made with graphite and bagasse-ash from Stir casting method. The author noted that as the percentage of reinforcement increased in the base alloy, the hardness of composites was gradually enhanced, composite ductility reduces with growing fuel content in the matrix alloy.

Yuanyuan Jin et al. (2019) [18] The author pursued F.S.P with aging therapy to improve the mechanical characteristics of AE42 as-cast. The author examined the grain size and mechanical properties of the composite. The author observed that the grain size reduces from 81 to 7.4 μm because of continuous dynamic recrystallization. The YS and UTS of the F.S.P specimen reduced relative to BM and considerably increased in elongation along the PD. However, the values of YS, UTS, and elongation along TD were considerably improved.

Mohammad Mohsin Khan et al. (2017) [19] fabricated ADC 12 alloy with SiC and fly ash by liquid metallurgy and seen the effect on hardness, M.S, density, and tensile strength. The author saw the hardness of composites was greater than alloy, the density of SiC composite was greater than Matrix but fly ash composite has less density and tensile strength of SiC composite was less than the base matrix and FA composite was greater than base alloy.

K.M. Mehta et al. (2019) [20] studied the wear behavior of reinforced Al-6061-T6 S.C made from Friction Stir Processing (F.S.P) with boron carbide (B4C). Two specimens were prepared with 1 pass for capping the groove and 3 were for stirring processing. In specimen-1, the direction of successive processing passes was the same. The sample was rotated 180° for successive processing passes, thus reversing the processing moves direction. From the experiment, the author observed that the specimen-1 wear was 72.15%

less than the base metal, while specimen-2 showed 74.82% less wear than base metal and 9.58% less wear than specimen-1.

Nagaraj N et al. (2018) [21] fabricated Al-7Si with F.A by stir casting method and observed the effect on microstructural analysis, hardness and U.T.S. The author contrasted the outcomes with the base metal and found that the Al-7Si-Fly ash composites showed greater durability and enhanced in the tensile characteristics relative to the base alloy Al-7Si.

Siddharth Patel et al. (2017) [22] studied the effect on tensile, compressive, yield strength, Hardness, and toughness of reinforced AL6061 with Fly ash and E-glass fiber by stir casting method. The author saw that tensile strength, yield strength, and compressive strength, percent elongation, and hardness rises through the addition of F.A with continuous E-glass fiber but only the 6 percent fly ash sample decreases in hardness. Only by adding the fly ash reduces toughness.

Sivanesh Prabhu et al. (2019) [23] The author reported improvement of the F.S.P AA6082/CaCO3 composite M.S (10-12 μm) as a result of dynamic recrystallization. This study the author was taken 2.5 N to 15 N load to report the wear and friction measurements of composite fabricated using F.S.P. He reports the reduction in grain size about 10-12 μm from 141 μm grain size, microhardness increased from 64 Hv to 87 Hv and the wear rate was reduced by 1/3 of AA6082 and 2/3 of F.S.P AA6082.

B. Ramgopal Reddy et al. (2018) [24] fabricated Aluminium 6082 with Silicon Carbide and Fly Ash by stir casting method and saw the effect on U.T.S, hardness, wear and M.S. Through this experiment the author saw an enhancement in the U.T.S, hardness and wear characteristics with a rise in the weight fraction of SiC and F.A reinforcement in an aluminum matrix.

T Satwash Kumar et al. (2018) [25] made composite by A356 with Bagasse Ash from Stir Casting method to compare mechanical properties with the base metal. The author noted an enhancement in the composites hardness, compressive strength, tensile strength and decline in impact strength with a raise in wt percentage of bagasse particles.

Shahrukh Shamim et al. (2017) [26] fabricated Al-Si-Mg-Ti alloy with eggshell particles by stir casting method to check the effect on elastic behavior, U.T.S, and fracture toughness. From this fabrication the found that as wt% of eggshell increased the tensile strength and Y.S get increased and weight and fracture toughness of the composite decreased.

Jingming Tang et al. (2019) [27] used F.S.P multi-pin tool to fabricate AA1060 aluminium alloy with SiC particles to investigate M.S, microhardness, and wear properties of the composite. In this study, the author did the experiment at 950 rpm of tool and 40 mm/min feed rate in the transverse direction and seen that the multi-pin tool produces more frictional heat and effect of a stir as compared with one pin tool. By the use of more than one probe tool, the author increased the microhardness, reduced the C.O.F and wear properties of the fabricated composite. The author also reported that as the size of SiC reduced and the wear type also changes from abrasive to adhesive wear.

Sumit Kumar Tiwari et al. (2017) [28] Manufactured Al7075 with F.A and E-glass to control the impact on M.P like hardness, tensile strength, compressive strength and yield strength by stir casting technique. The author observed from the experiment that the tensile strength enhancement, compressive strength, hardness as we raise the fly ash weight proportion and there was a reduction in ductility with a percentage increase. With increased particle size of fly ash, tensile strength, compressive strength & hardness reduces.

N. Yuvaraj et al. (2016) [29] have used the B_4C and TiC as a reinforcement material to fabricate the composite by using AA5083 from F.S.P. The author studied the effect on mechanical properties and tribological properties. The author noted that F.S.P composite samples (mono and hybrid) displayed uniform dispersion of matrix reinforcement particles and greater hardness and strength than the alloy F.S.P Al. Compared to Al – TiC and Al – B_4C / TiC, Al – B_4C nano-reinforced composite displayed the greatest hardness and tensile strength. Compared to B_4C composite, Al – B_4C / TiC discovered greater wear strength and low hardness.

Narayana Yuvaraj et al. (2015) [30] fabricated the composite by F.S.P from nano and micro B_4C reinforcement in AL5083 and studied the effect on M.S, wear and UTS. The author observed that as the number of passes increases, hardness, UTS, and wear rate

increases and grain size become finer. B_4C nanoparticles give ultra-fine grain size. Wear properties improved by the addition of nanoparticles as it compared with microparticles.

Honglong Zhao et al. (2019) [31] saw the effect on M.S of weld nugget (WN) of aluminium 6063 alloys. The grain size was finer at the bottom than the upper zone. The author observed tunnel defects at low speed i.e 300 rpm in the thermos mechanically affected zone (TMAZ). When the rotation speed exceeds 700 rpm, it was possible to create a good interface between the WN and the TMAZ. When RPM of the tool was low, the UTS for both single and double F.S.P passes were lower than the base material (BM) but as velocity increases, the UTSs gradually improved and then higher than the BM.

2.1. Conclusions from Literature Review:

1. The AA and its composites have numerous engineering application, moreover the MMC of AA can be manufactured using various processes like FSP, Stir Casting, Ultrasonic Casting.
2. FSP being the green manufacturing process have minimum waste, no harmful emissions and can be used for variety of MMC.
3. The environmental waste can be used for reinforcement for the MMC.
4. The MMC manufactured by FSP showed improved mechanical and tribological behavior.

2.2. Literature Gap

There is not much work on the study of pre heating of materials before FSP and its impact on the mechanical and tribological properties.

The researchers used the materials as composite for MMC of AA which were not cost effecting.

The DOE has not been observed for mechanical and tribological investigation.

2.3. Research Objective

- Selection of suitable material and process for MMC.
- Investigation of mechanical properties of MMC and comparison with the unprocessed AA.

- Investigation of morphological behavior of MMC and comparison with the unprocessed AA.
- Investigation of tribological properties of MMC and comparison with the unprocessed AA.

2.4. Methodology

1. Comprehensive literature survey for the selection of materials and process for manufacturing MMC.
2. Sample preparation and selection of process parameters for FSP.
3. Investigation of micro-hardness, tensile strength and micro structure of the processed and unprocessed samples.
4. Investigation of tribological properties according to the L9 orthogonal Array.
5. Comparison of mechanical and tribological behavior of MMC of AA and unprocessed AA.

CHAPTER 3

EXPERIMENTAL SETUP AND PROCEDURE

The experiment was carried out to investigate the mechanical and tribological properties of composite material. It required the test specimen of aluminium based alloy.

3.1. Materials

The experiment was carried out on Al6063 (200×75 mm) plates. The chemical composition of Al6063 was shown in Table 4. The compositions were verified by chemical spectroscopy.

Table 4 Chemical Composition of AA6063 Material

Elements	Si	Fe	Mg	Mn	Ti	Zn	Ni	Cr	V	Sr	Al
Mean	0.64	0.2732	0.6941	0.1074	0.0736	0.0693	0.039	0.0345	0.035	0.0005	98.01

The microparticles of marble dust were used as reinforcement to enhance the properties of Al6063.

To observe the effect and advantages of F.S.P, the experiment and analysis were divided into the following steps: -

- F.S.P experimental setup.
- Formation of the Tool and workpiece for F.S.P.
- Packing the groove by marble dust.
- Processing on the F.S.P machine.
- Wire cut of test samples.

3.2. Experimental Setup

Friction Stir Welding machine was used for processing of Al6063. Figure-5 shows the FSW machine which was used for fabrication. Table 5 shows the full specifications of the FSW machine which was used for fabrication of composite. This machine consists of a 3 phase powerful motor which drives the F.S.P tool and provides the efficient torque to it. The machine has the system were semi-automatic. It has a hydraulic system which makes

it efficient to use and work with accuracy. The hydraulic system was used to clamp the w/p, up and down motion of the tool and the transverse motion of the base. The discharge of the hydraulic was controlled by the actuators using a nob. This affects the motion of the tool and the base plate. The F.S.P machine used to fabricate the composite and detailed view of the machine was shown in Figure 5.

Table 5 FSW Machine full specification

Machine Specification	
Machine Size(L×B×H)	1300×1650×2000 mm
Table Working Surface	600×400 mm
Machine Total weight	2 Ton
Welding Materials	MS, Al, Cu
Job Size Maximum (Thickness)	5 mm
Welding Geometry	Straight
Machine travel	
x-axis	600 mm
y-axis	200 mm
z-axis	300 mm
Axis thrust force	
x-axis	250-2500 Kgf
y-axis	400-4000 Kgf
Motion	
x-axis travel speed	0-5000 mm/min
y-axis travel speed	0-2000 mm/min
Spindle Housing	
Spindle	Iso 40 taper
Spindle speed	1440 rpm(max)

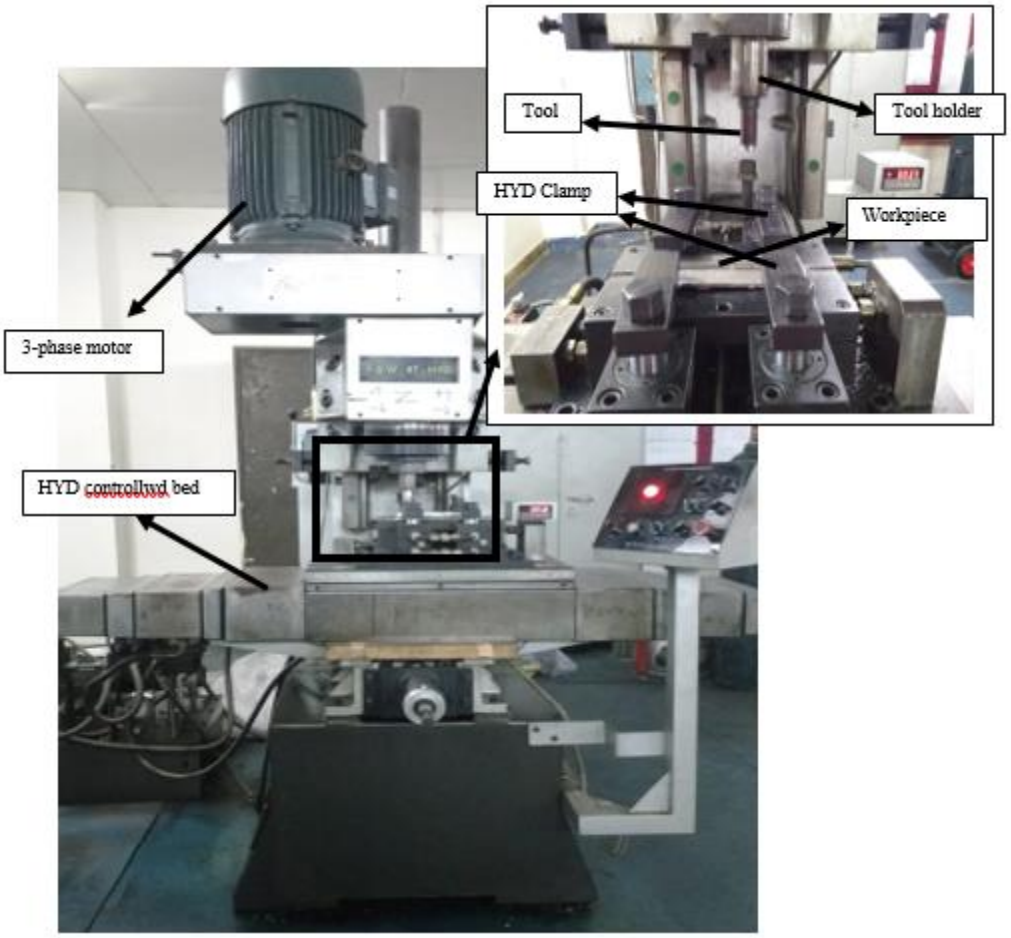

Figure 5 F.S.P Setup

Various F.S.P process parameters which were used to change the properties of the material. These parameters were changed from material to material for better processing. FSW machine can fabricate the composite on different process parameters which were shown in table 7.

Table 6 Process parameters

Rotation speed(N) RPM	**Feed Rate (F) (mm/min)**	**Tool angle(A) degree**
1400 (Max)	1800(max)	0^{O}-7^{O}

3.3. Formation of The Tool and Workpiece for F.S.P

3.3.1. Workpiece Formation

To work on the FSW machine 200×75 mm^2 plate was required. To make the proper dimensions of the plate Power Hacksaw and milling machine was used.

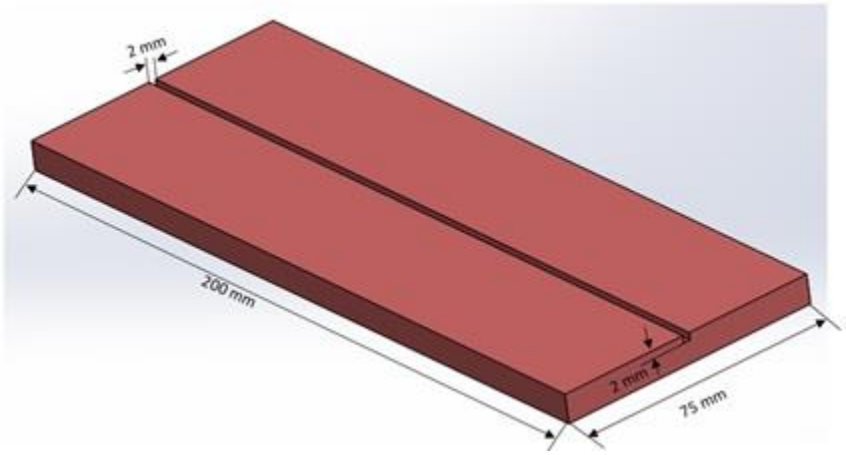

Figure 6 Al6063 plate with 2×2 Groove

For the fabrication of the composite and to enhance its properties of the base material, reinforcement was used. This reinforcement was filled in between the plate by cutting the grove on the base plate. The grove of 2×2 mm was created by universal milling at the center of the plate for processing. The aluminium plate with a groove as shown in Figure 6 by using solid modeling.

The Dimensions of the groove as shown in table 7.

Table 7 Groove dimensions

Depth	2 mm
Width	2 mm
Length	200mm

3.4. Tool Formation

From the literature review and the trial work, triangular pin tool was selected for the experimental work.

Following were the advantages of the triangular tool over cylindrical tool:

- It provides better processing results
- The mixing of base material with reinforcement was better.
- Due to increased interface between the pin and the plasticized material, the heat generation was more by triangular pin.

The tool was made from Mild steel. By using CNC lathe facing and turning was done and end milling machine was used to make a triangular section tip. The slot was cut over the face of the tool for better gripping and to avoid slipping of the tool while doing F.S.P. The designed tool by solid works and the fabricated tool as shown in Figure 7.

The tool used for F.S.P consists of the tip and the shoulder. The diameter of the shoulder was 19.95 mm, the height of the tip was 5 mm, the tip of the tool was equilateral triangle shape with equal sides of 6mm. Table 8 shows the full dimensions of the F.S.P tool.

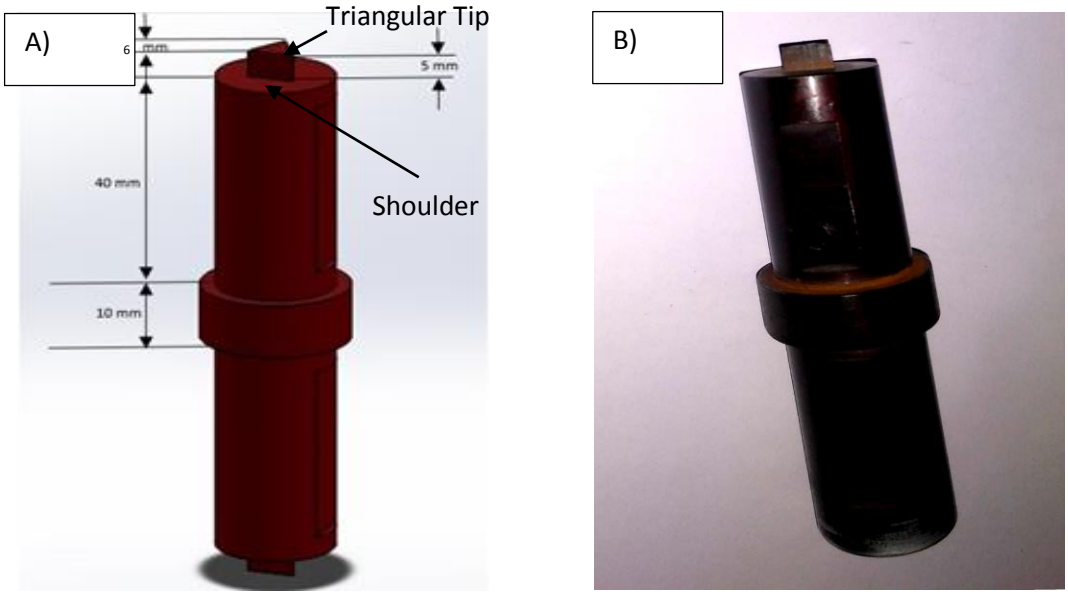

a) The designed tool on SolidWorks, b) fabricated tool by lathe and milling

Figure 7 F.S.P Design Tool

Table 8 Tool Dimensions

Tool Length	100 mm
Shoulder Diameter	19.95 mm
Pin Width	5 mm

Pin Dia	7 mm
Pin type	Triangle

3.5. Processing Methodology

3.5.1. Friction Stir Processing

Friction Stir Processing was carried out with the help of the FSW machine. The groove (2×2) was created on the AA6063 plate by the milling machine and the composite was fabricated, by using FSW machine. The groove was properly cleaned by using acetone and the pre-heated marble dust particles were filled and closed by the closing method. The marble dust was preheated at a temp 150^{o}C to eliminate the moisture content and air so that mixing should be proper. In the groove closing method, the groove was filled by marble dust and then it was closed by F.S.P probe less tool to prevent escaping of the micro-particles. The principle of frictional heat was used for closing of the groove. The frictional heat was generated by the phenomenon of the rubbing action between tool probe less tool and the w/p. After the closing of the material, the plate was subjected with the help of F.S.P tool with the probe as shown in Figure 8. On the basis of literature review, F.S.P parameters were selected to carry out the experimental work. Table 9 shows the process parameters.

Table 9 Processing parameters

Sample	**Material**	**Feed rate (mm/min)**	**Tool angle (Degree)**	**Rotational speed (RPM)**	**Preheat temperature(^{0}C)**
1	Base Material	-	-	-	-
2	AA6063/MD	25	0^{0}	900	Room temp
3	AA6063/MD	25	0^{0}	900	100
4	AA6063/MD	25	0^{0}	900	200

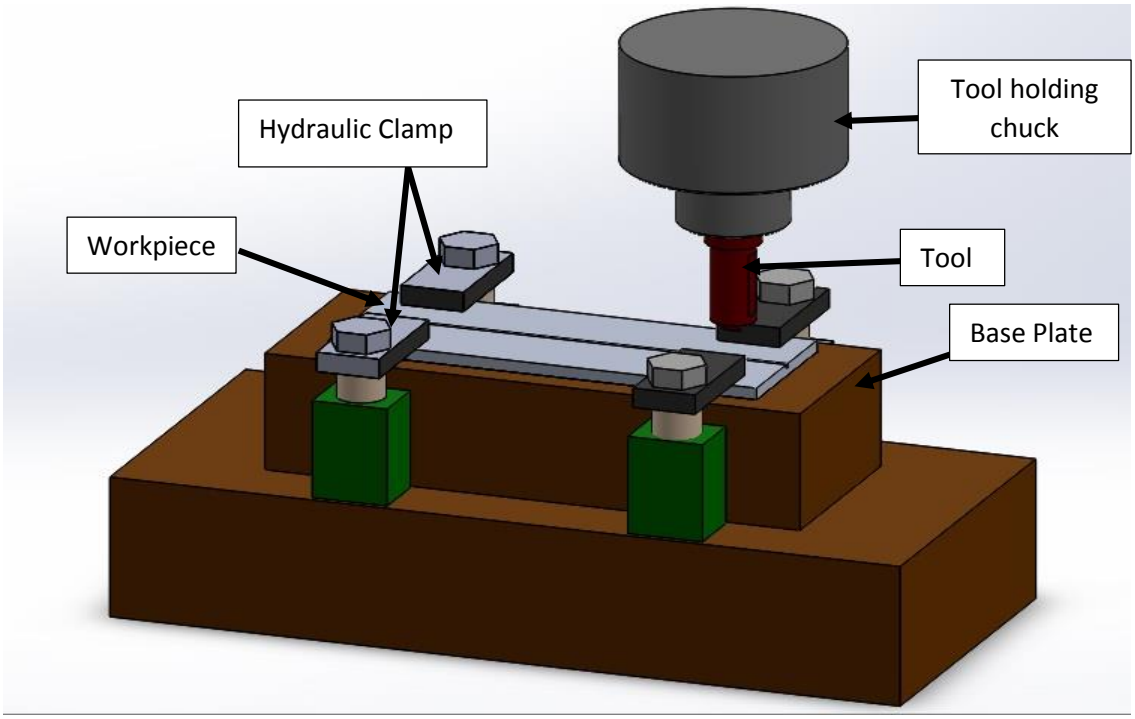

Figure 8 Setup of F.S.P

The stepwise procedure of producing the composite was shown in Figure 9.

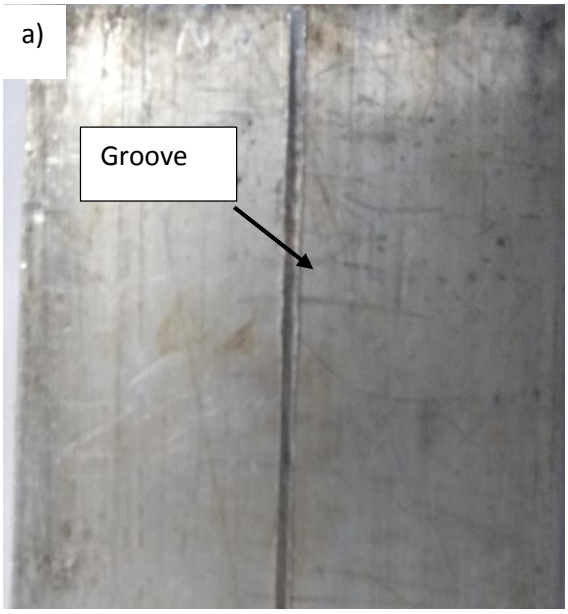

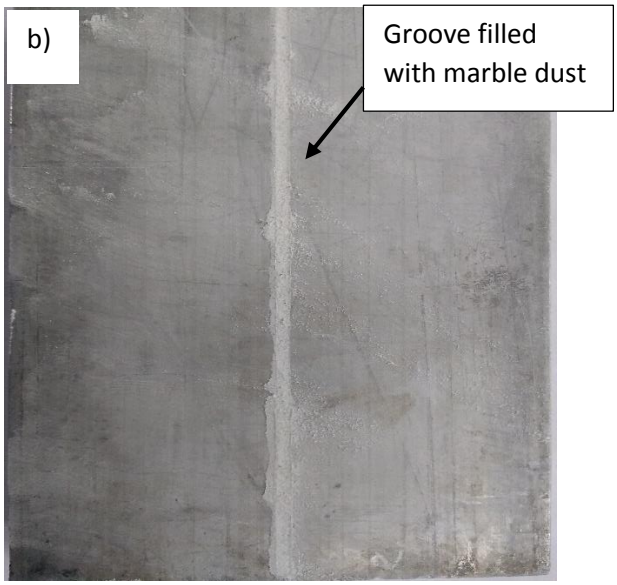

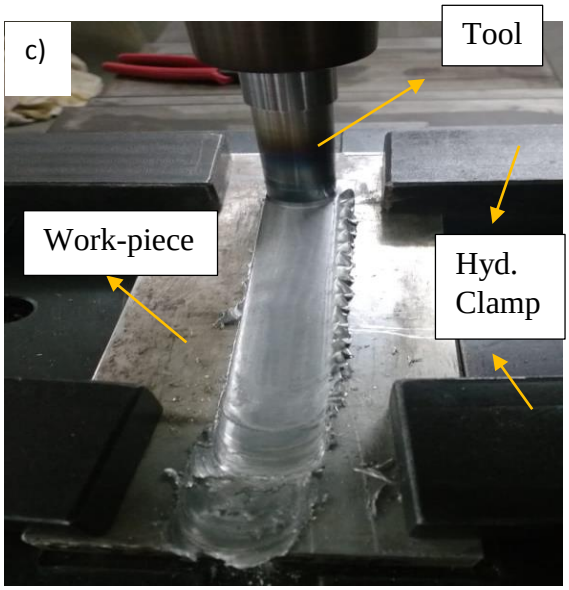

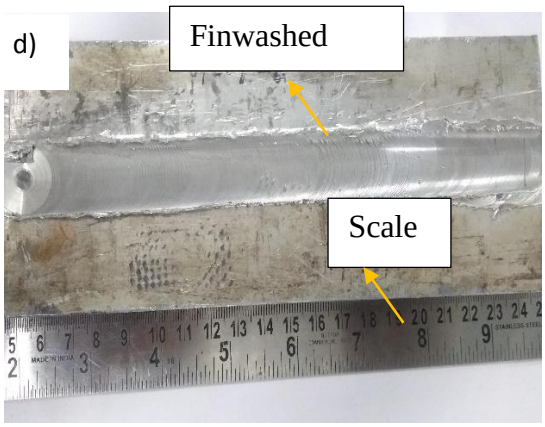

a) Groove without reinforcement.

b) Groove filled with reinforcement.

c) Closing of material with prob-less tool.

d) Processed material by the triangular probe.

Figure 9 F.S.P Process Methodology

3.6. Sample Preparation: -

To study the mechanical properties, M.S and tribological properties of the samples were cut parallel to the F.S.P processed zone with the help or Wire EDM as shown in figure 10 and Figure 11 shows the final blank and pieces after cutting process by wire EDM.

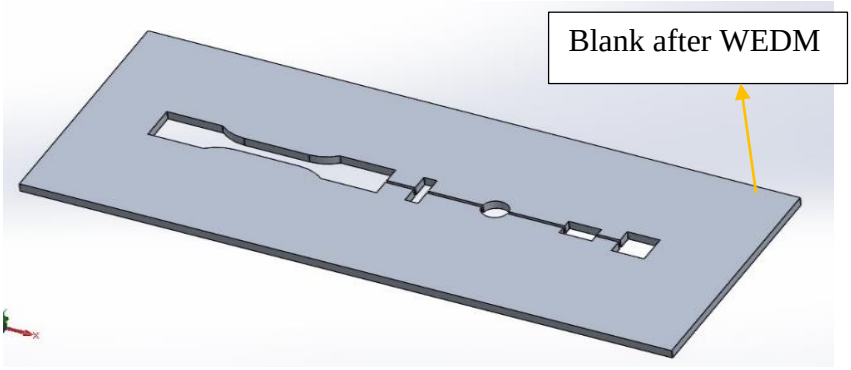

Figure 10 sample cutting by Wire EDM

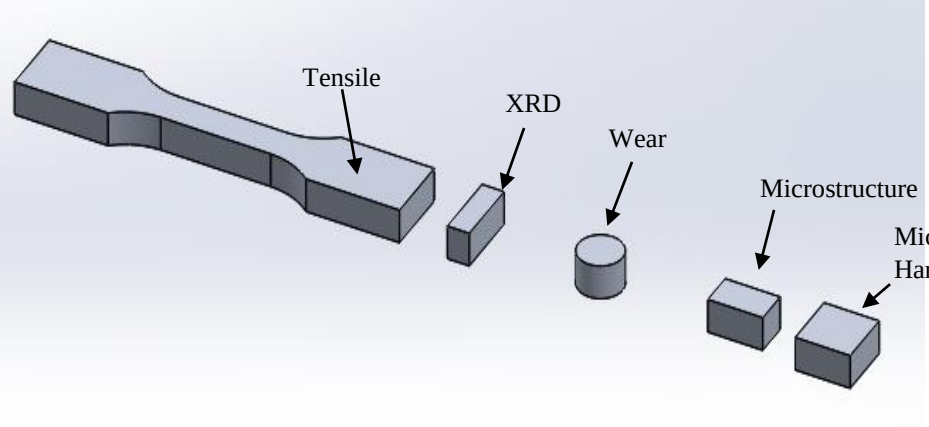

Figure 11 Samples after wire EDM

3.6.1. Tensile Specimen

The tensile specimen has prepared as per ASTM standard and the samples were taken along the processed surface in the F.S.P direction by the wire EDM machine. Figure 12 shows the tensile specimen with full dimensions for testing UTS, elongation and tensile specimen after wire cut.

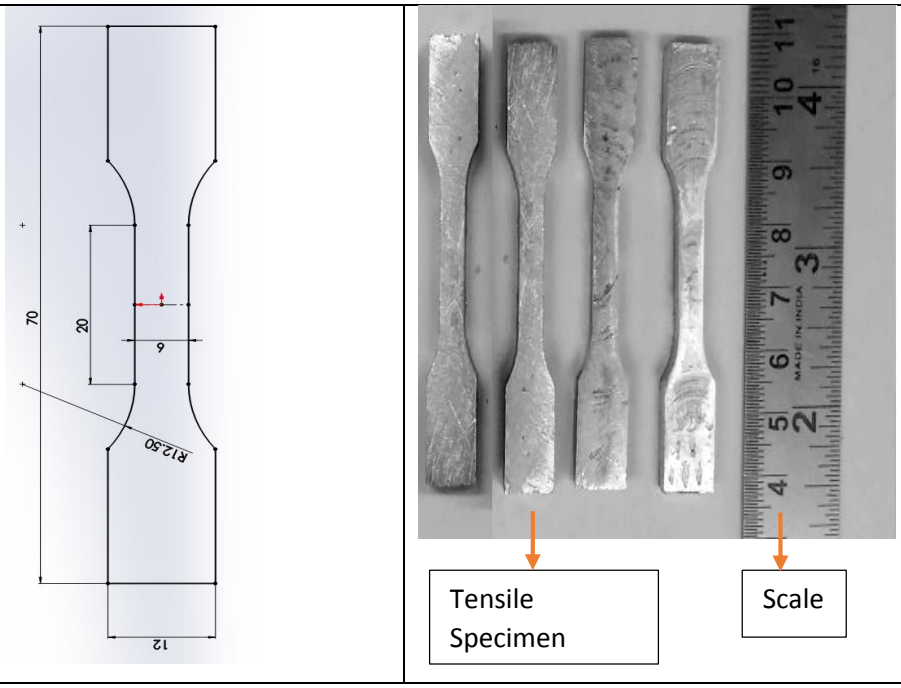

a) Tensile Specimen with full dimension by AutoCAD.

b) Tensile specimen after cutting

Figure 12 Tensile Specimen

The tensile test has carried at 1mm/min strain rate at room temperature on computer controlled UTM (Tinius Olsen) H50KS as shown in Figure 13. Ultimate tensile strength and percentage elongation were recorded.

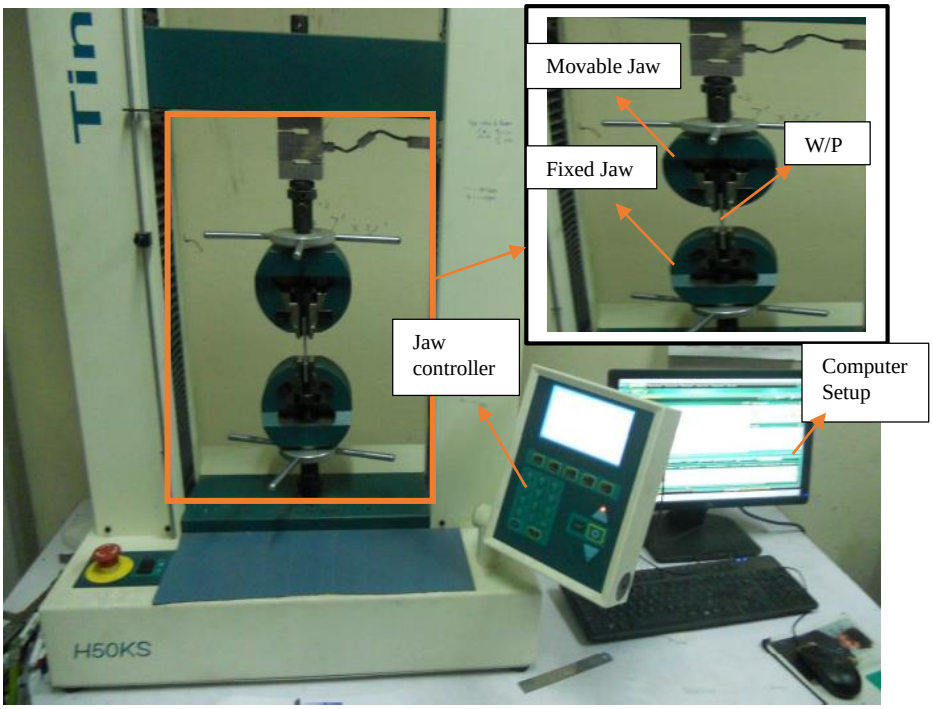

Figure 13 UTM Machine, DTU

3.6.2. Micro Hardness

The Microhardness test was carried on FWASCHERSCOPE HM2000 microhardness tester machine. Figure 14 shows the machine setup. Table 10 shows the full specification of the machine. Prior to this experiment, samples were polished from 100 to 1200 grit fine emery paper to remove the oxide layer and other scales from the surface. This was done so that the indentation mark should be properly visible, Figure 15 shows the polished samples to measure Vicker's hardness. The Vickers microhardness values were taken using the load of 300mN with a dwell time of the 20s on the processed regions.

Figure 14 Vicker's Hardness Machine Setup

Specification of FWASCHERSCOPE HM2000 Machine:

Table 10 Machine Specification

Hardness	**Load**	**Dwell Time**
20Hv to 1500Hv	10mN to 1000mN	20sec

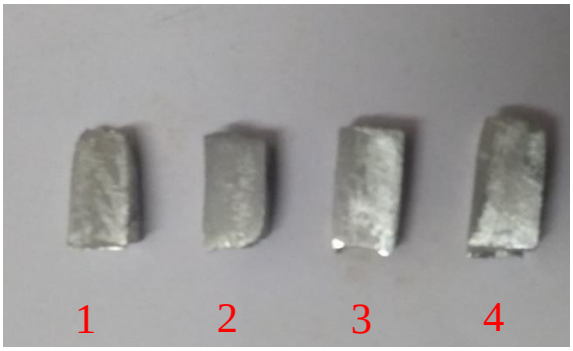

Figure 15 Micro Hardness pieces

3.6.3. Microstructure

The samples were cut from the specimen by wire EDM, the surface of the specimen was polished, etched for M.S on an optical microscope. For holding and proper polishing of the samples, cold mounting with resin and hardener was done. Without mounting of the samples the pieces were not held and they also get unbalance. After mounting the samples were polished using 100, 120, 220, 320, 400, 600, 1200, 2000 grits ambry paper. After that, wet polishing was initially done by contacting the samples with fine grit emery paper against the rotating disc. Lastly, polishing was done on a proprietary cloth using alumina powder shown in Figure 16. Also, intermittent sample drying was carried out by the hand dryer supplied in the machine. Lastly, ethanol was used to wash the surface to remove contaminants. The samples were etched using Keller's reagent solution to unveil the grain structure. After the chemical etching, the left over layer on the surface of the metal was removed by submerging it in ethanol. During the F.S.P, microstructural development was characterized by an O.M, with software for image analysis, the microscope was with 100, 200, 500 and 1000 lens and computer. M.S of base metal, 4 F.S.P processed pieces have seen using OM. Figure 17 shows the polished samples cut from the F.S.P zone for M.S study.

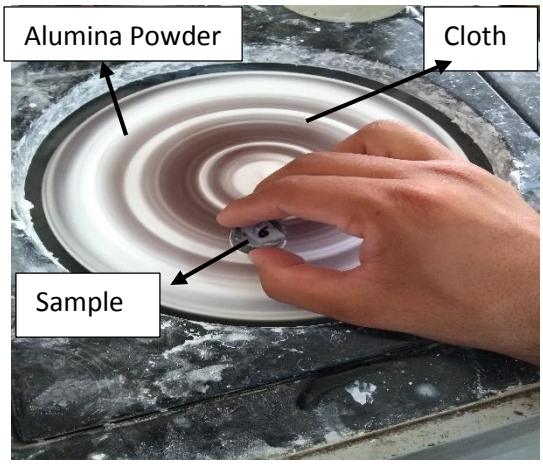

Figure 16 Wet polishing with Alumina

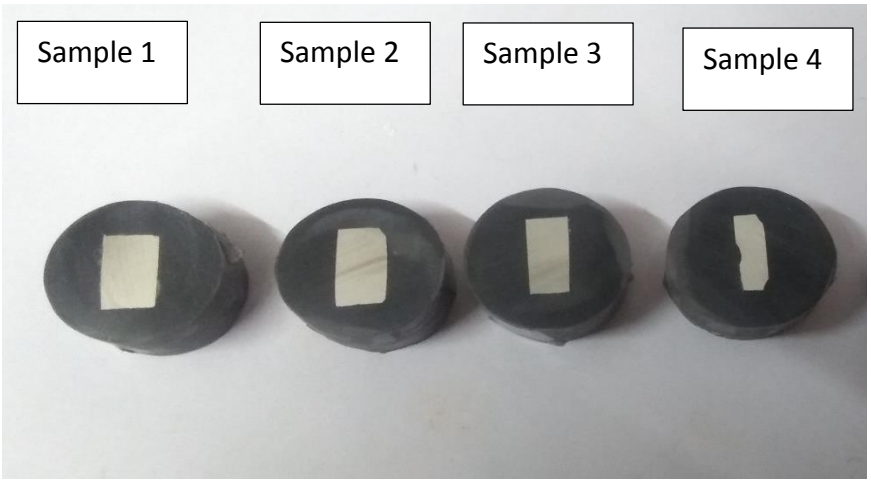

Figure 17 Microstructure Specimen

3.6.4. X-Ray diffraction(XRD)

XRD works on the principle of constructive interference of monochromatic X-ray. The X-rays were focused and aimed at the sample. The interaction of the incident ray with the sample results in constructive interference (and a diffracted ray) when conditions fulfill the law of Bragg (nπ=2dsin). This law refers to the wavelength of electromagnetic radiation to the diffraction angle and the lattice spacing in a crystalline sample.

The XRD samples were shown in Figure 18. The XRD was done for characterization of the composite material and the base metal to compare the mixing of reinforcement. After

cutting the samples polishing was done with the help of fine ambry paper to eliminate the roughness and to make even surface.

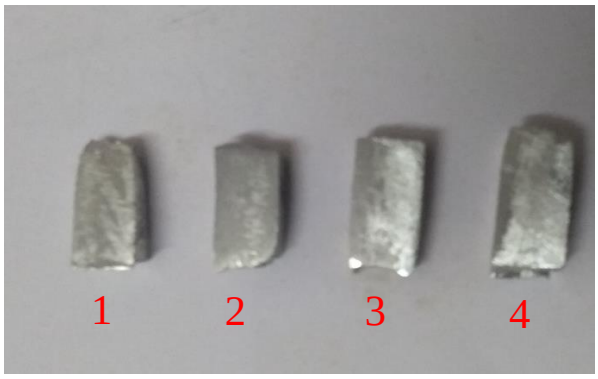

Figure 18 XRD Samples

3.6.5. Tribological Testing

3.6.5.1. Sample Preparation

- The samples of 8mm Diameter were cut for wear test from the stirred zone by wire EDM. The male-female fitting were made to hold the 4mm pins. For the fitting of the pins the hole on the pins was drilling with 2.5 mm deep and 3 mm in diameter and male part was made of 3.10 mm in diameter of the mild steel rod of 10 mm diameter. These pieces were connected as Interference fit and also pasted by Araldite tube (adhesive used for pasting) so that it will not come out between the test. After pasting these specimens left for 24 Hr for drying and for good bonding. Figure 19 shows preparation of the sample.

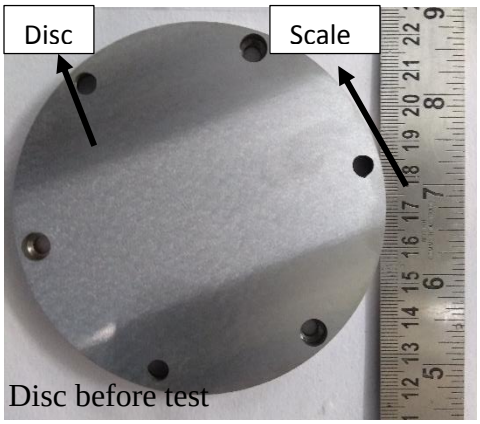

Disc before test

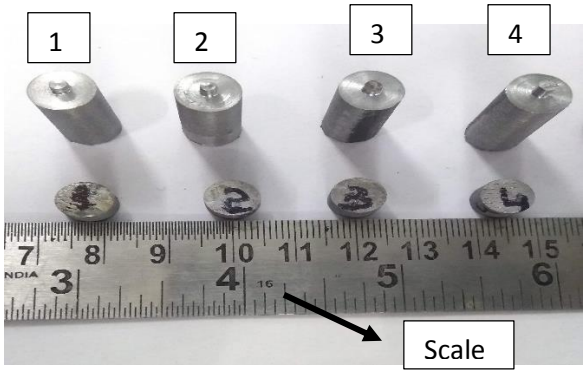

Wear Specimens

Figure 19 Wear test preparation

The sliding wear test was carried out using pin-on-disc tribometer ASTM-G-99. Wear of the pins has seen by running 500m fixed distance on 100mm EN-31 disc with about 60HRC. Wear test parameters were shown in table 11.

Table 11 Wear Parameters

Disc temperature(ºC)	50	100	150
Disc Speed(RPM)	300	500	700
Sliding Distance(m)	500	500	500
Load(N)	20	30	40

Before starting the test initially and after every test the weight of the pins was noted down to calculate the wear rate.

Figure 20 shows the pin and disc condition after the test.

The time was dependent on the track diameter and the disc rotation.

Calculation of time per wear test was

Specimen track diameter = x mm;

Disc Rotation = y rpm

Circumference of track = πx mm;

πx mm was the distance traveled by pin in one rotation,

Distance traveled in 1 min = $\frac{\pi x}{1000} \times y$ meter

Time for one test = $500 \Big/ \frac{\pi x}{1000} \times y$ min

Wear specimens after test

Figure 20 pin and disc after the wear test

RESULTS AND DISCUSSION

This chapter deals with the effects of F.S.P on microstructure, microhardness, U.T.S, wear properties of the AA6063/Marble dust composite.

4.1. Mechanical Testing

4.1.1. Micro-hardness

The micro-hardness was examined on Fischer micro-hardness tester. The Vickers hardness of the specimen was calculated by taking an average of 10 readings on the samples. The micro-hardness values in case of AA6063 were recorded as 67.29 Hv and the micro-hardness in case of the composite prepared at 200^{O}C pre-heat temperature was 77.396 Hv, this increment was about 15% from the base material was due to the presence of CaO, SiO_2, MgO, and Al_2O_3 [49,50]. The hardness was increased because of the compact or finer grain structure at a higher temperature and may be due to the presence of Al_2O_3 as evident in XRD results. The hardness of the samples was shown in figure 21.

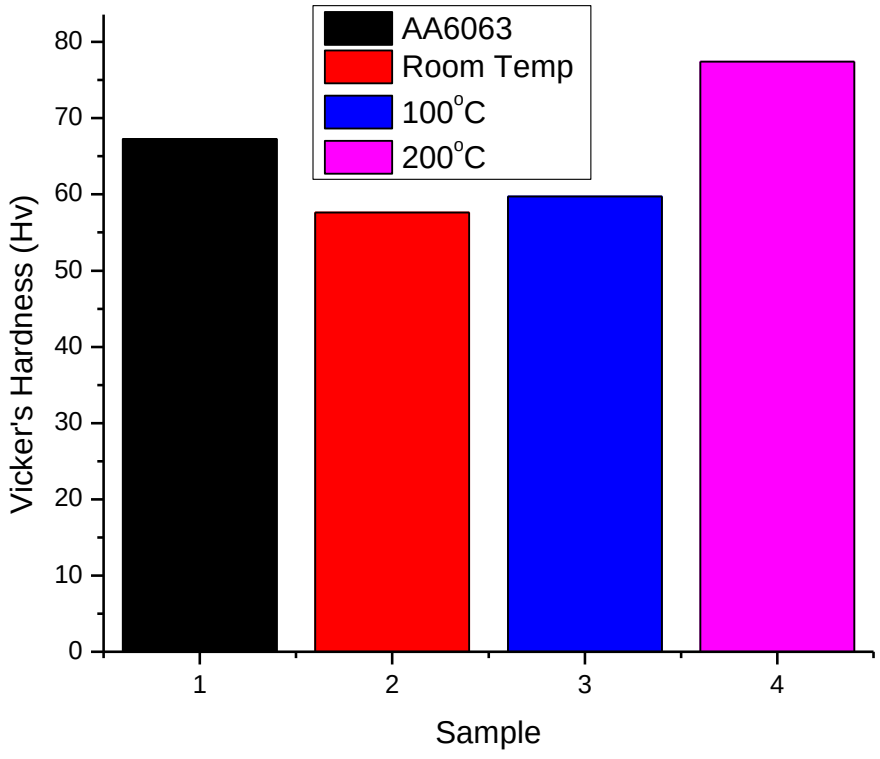

Figure 21 Vicker's hardness Bar Chart

4.1.2. Tensile Strength

The tensile strength of AA6063 was 157 MPa and the U.T.S of sample 4(pre-heat at 200^{o}C) was 202 MPa. There was an increment in U.T.S about 29% from the base material. The U.T.S increases with increase in pre-heat temperature of the specimen before F.S.P. Figure-21 shows the U.T.S of the specimens. MD particle can lead to an increase in tensile strength, may be due to the excellent impact strength, wettability and excellent bonding between the matrix. The loads applied were transmitted in the composite to the MD particles, which increases the load-bearing capacity [51-53]. Elongation was also increased from 6.5mm for AA6063 to 7.2mm F.S.P at 200^{o}C. There was an increment of about 9.7% from the base material. Table-13 shows elongation values of all samples.

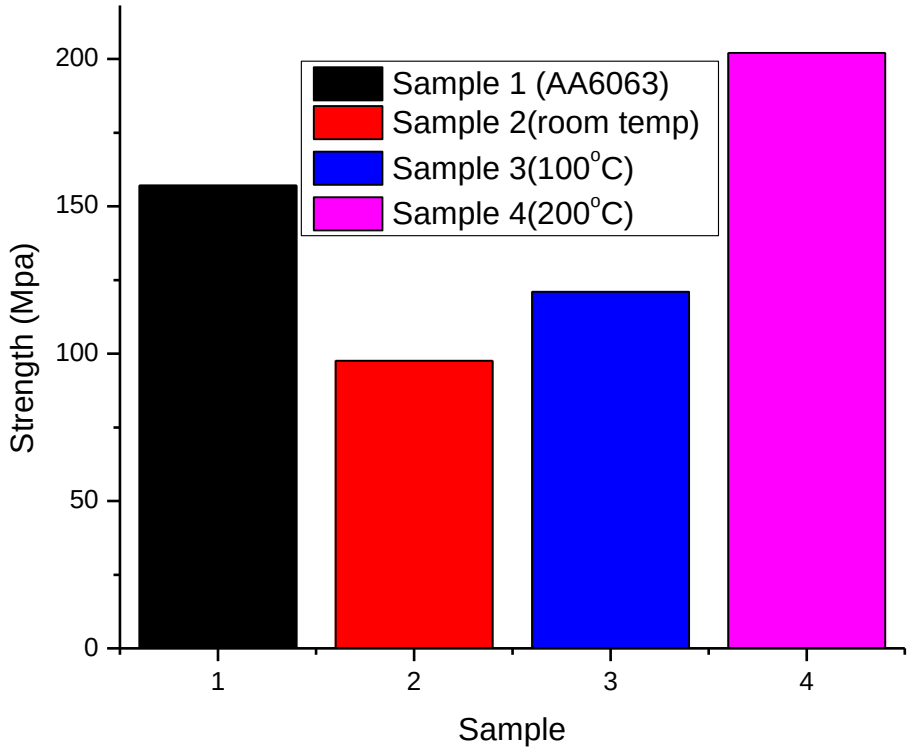

Figure 22 UTS of all Samples

Table 12 strength and elongation of the specimen

Specimen	Strength(Mpa)	Elongation(mm)
Sample-1	157	6.5

Sample-2	97.6	2.7
Sample-3	121	1.8
Sample-4	202	7.2

4.2. Characterization

4.2.1. Microstructure

F.S.P results in the successful fabrication of AA6063/Marble Dust surface composite. The below Figure shows the optical microscope images at 500x and 1000x of the different specimen. Figure 23-26 shows the grain structure of sample-1, sample-2, sample-3, and sampl-4. M.S (a) figure shows M.S at 100x and (b) figure show M.S at 1000x.

These Figures reveal the shape of the M.D, as it was clear from the microstructure figures the marble dust was present in the composite with irregular shapes.

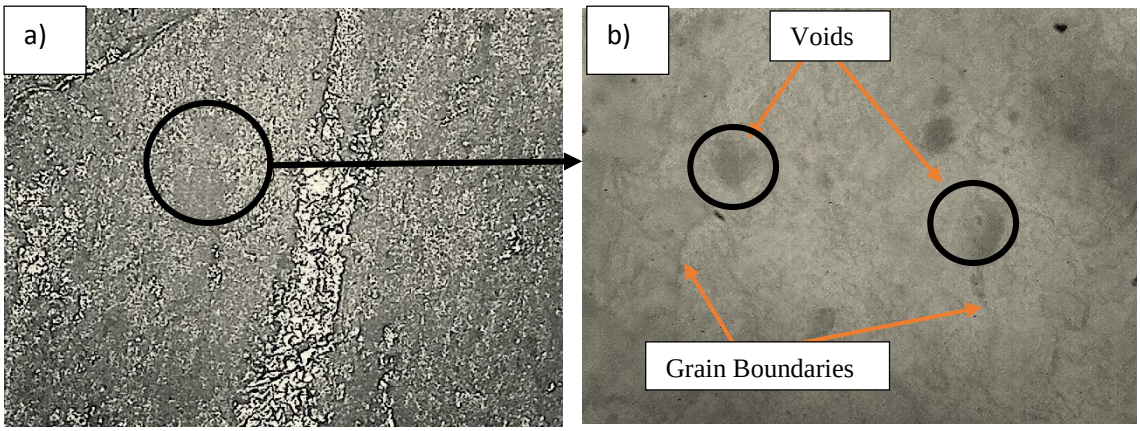

Figure 23 Micro-structure of Base Material

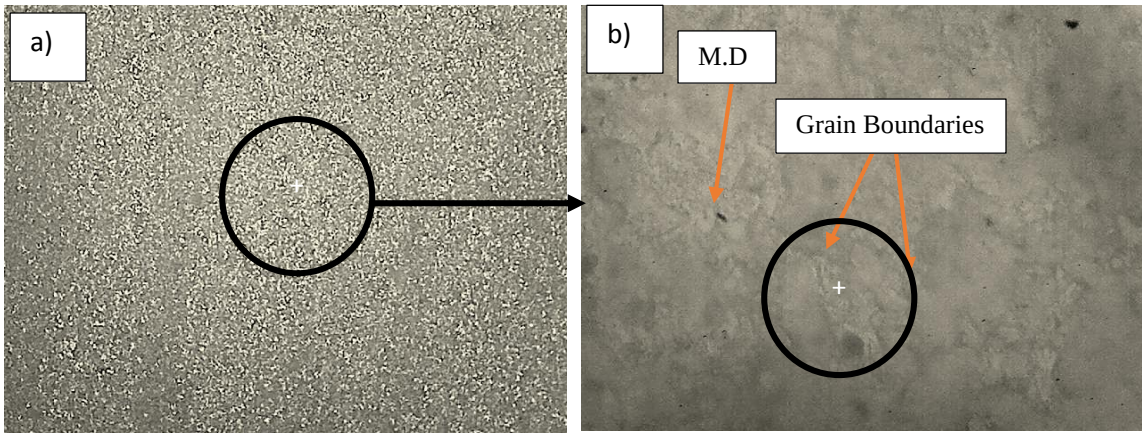

Figure 24 Micro-structure of Sample 2

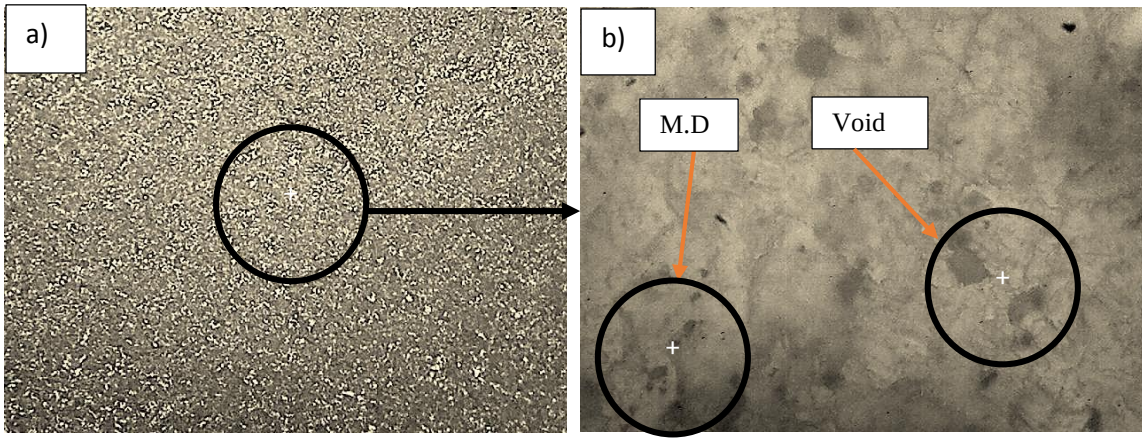

Figure 25 Micro-structure of Sample 3

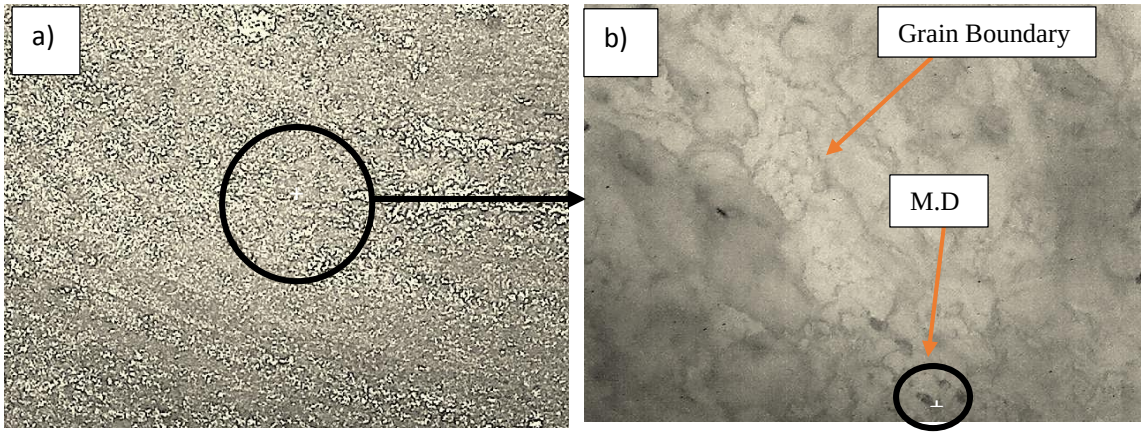

Figure 26 Micro-structure of Sample 4

4.2.2. X-Ray Diffraction

The XRD was done for the detection of the intermetallic compound of the samples. The rays are subjected at a range of 2theta angle from 10^{o}-80^{o} throughout the analysis. The peaks are detected in this analysis The results reveal the particles present in the sample of the AA6063 and in the processed samples. XRD results show that the major element in AA6063 was Al and Al-Fe-Si. The XRD of AA6063(Sample-1) was shown in Figure-27 (a) and the composition of marble dust shown in Figure 27(b) shows.

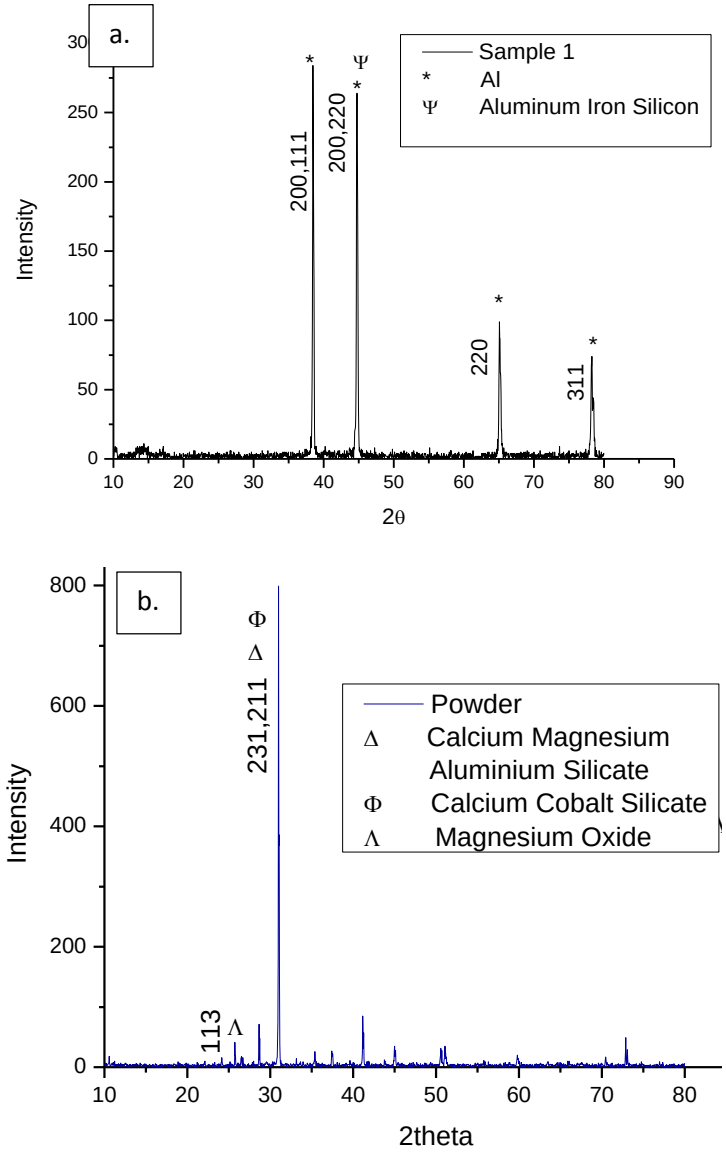

Figure 27 XRD of AA6063 and Marble dust

Figure 28 shows the elements like Ca, Si, O, Al, and Mg which proves the presence of M.D in the composite. The bonding between the M.D and the Al was shown in M.S. The XRD results also show that aluminum reacts with the atmosphere to form its oxide. Ca-Mg-Si was the main element formed in marble dust from the reaction. Ca-Mg-Si was seen at a 31^{o} 2theta angle.

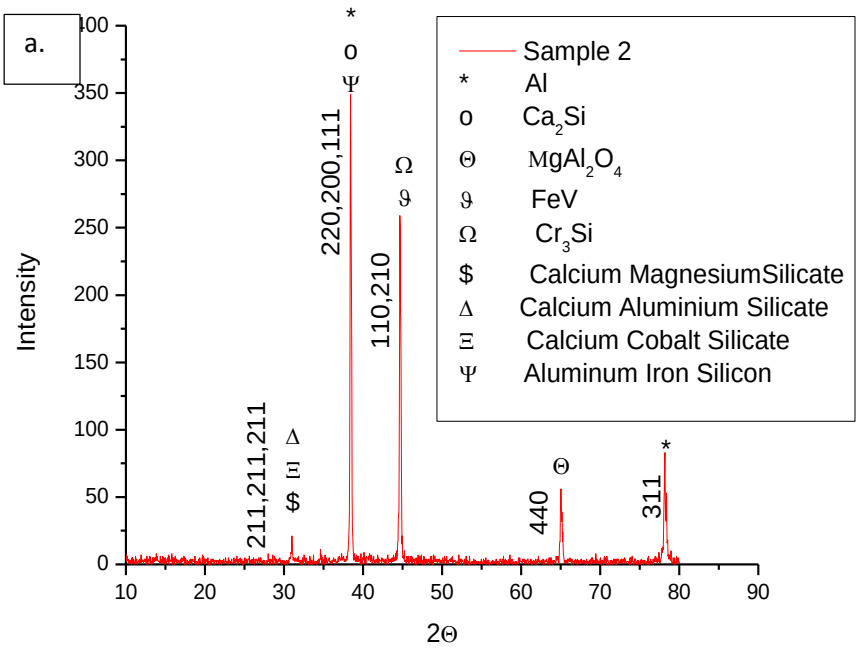

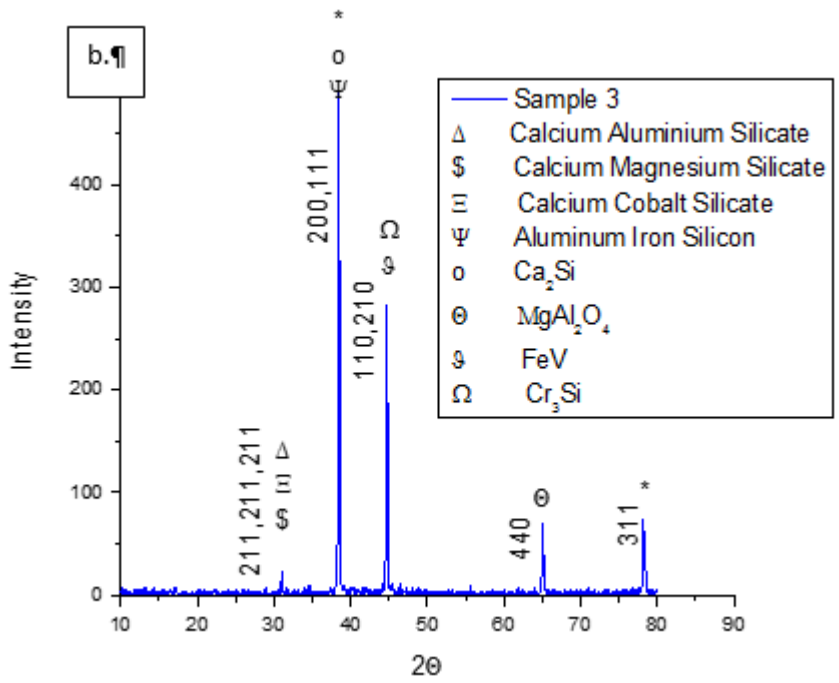

a. XRD of sample-2(F.S.P did at room temp).

b. XRD of sample-3(F.S.P did at 100^{o}C pre-heat temp).

Figure 28 XRD of sample-2 and sample-3

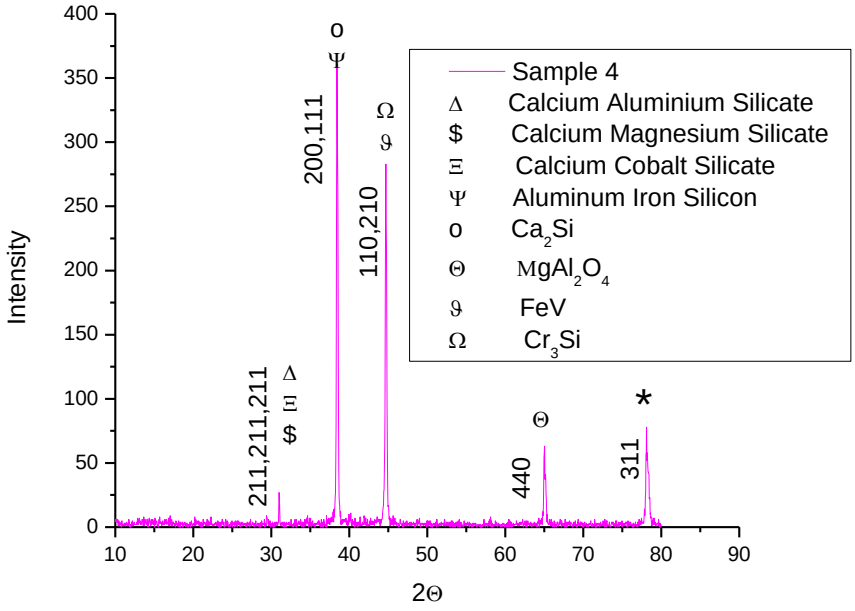

Figure 29 XRD of sample-4(F.S.P did at 200^{o}C pre-heat temp.)

4.3. Tribology testing

4.3.1. Design of Experiment (DOE) Of Tribo-Testing

Tribological investigation was done on AA6063 and AA6063/marble dust composite. The comparison was made b/t the samples, and the parameters were optimized. The input parameters were taken into consideration were speed, load, and temperature and the output parameter were specific wear rate and coefficient of friction. Tribological behavior is the function of the input parameters, which affects the properties of wear [55]. DOE of the tribology testing of Aluminium base material (Sample-1) was shown in Table 13 and table for processed samples shown in Table 14.

Table 13 Array for Sample-1

S.NO	Tool Rotation (RPM)	Load (N)	Temperature (K)
1	300	20	50
2	300	30	100
3	300	40	150
4	500	20	100
5	500	30	150
6	500	40	50
7	700	20	150
8	700	30	50
9	700	40	100

Table 14 Array of processed samples

Sample	Tool Rotation (RPM)	Load (N)	Temperature (K)
Sample-2	300	20	50
Sample-2	500	30	100

Sample-2	700	40	150
Sample-3	500	40	50
Sample-3	700	20	100
Sample-3	300	30	150
Sample-4	700	30	50
Sample-4	300	40	100
Sample-4	500	20	150

4.3.2. Analysis of tribology using Taguchi

The test was done according to the arrays shown in Table 13 & 14. The weight of the samples was measured initially and after every test. Figure 30 shows the SWR and COF of the base material (Sample-1). The COF was calculated by the tribometer setup and the SWR was calculated by the change in weight after successive tests.

4.3.2.1. COF of AA6063: -

The tribological investigation of POD was done and COF was calculated for the base material (AA 6063). The COF increases as the load and the speed increased as shown in Figure 30 (b). moreover, the temperature of the tribological investigation also affected the COF of tribo-pairs. The increase in temperature decreases the COF up to 100^{o}C but as the temperature was increased to 150^{o}C the COF increased as shown in Figure 30 (a). The response table is shown in Table 15 shows that speed has a maximum impact on the COF followed by temperature and lately by the load. The Taguchi analysis shows that the optimum parameter for COF was at a speed of 300rpm, a load of 20N and at 100^{o}C temperature as shown in Figure 31.

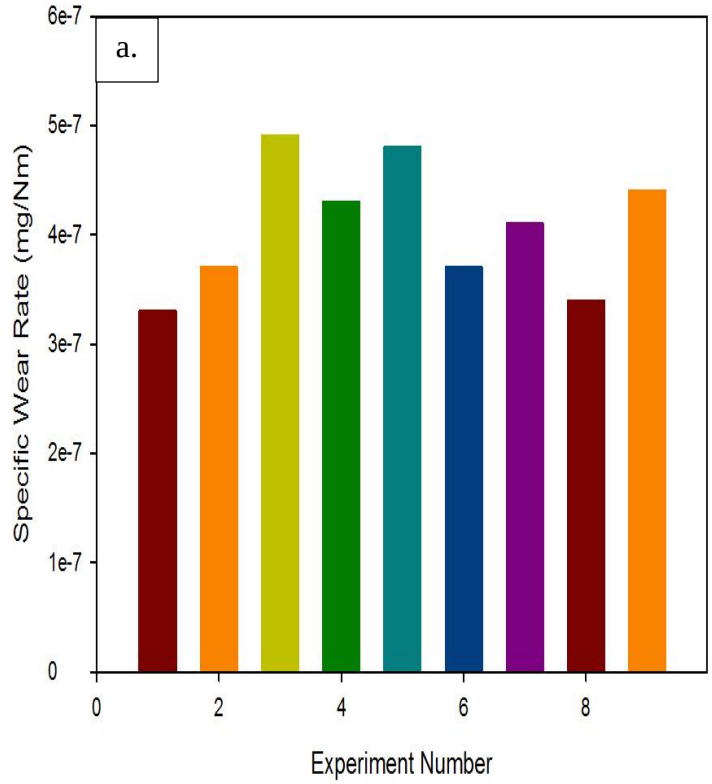
a.
6e-7
5e-7
4e-7
3e-7
2e-7
1e-7
0
Specific Wear Rate (mg/Nm)
0
2
4
6
8
Experiment Number

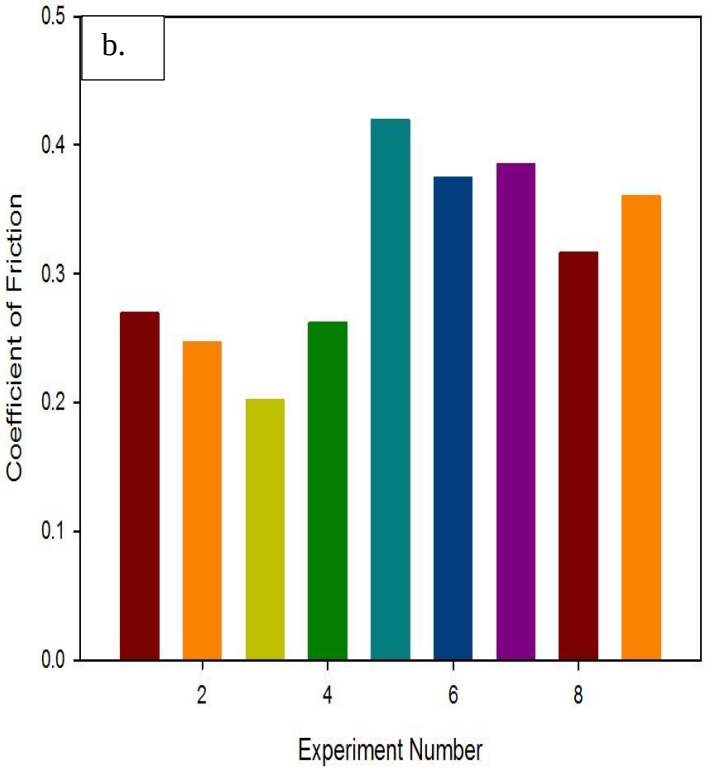
b.
0.5
0.4
0.3
0.2
0.1
0.0
Coefficient of Friction
2
4
6
8
Experiment Number

a. AA6063 SWR

b. AA6063 COF

Figure 30 AA6063(sample-1) COF Graphs

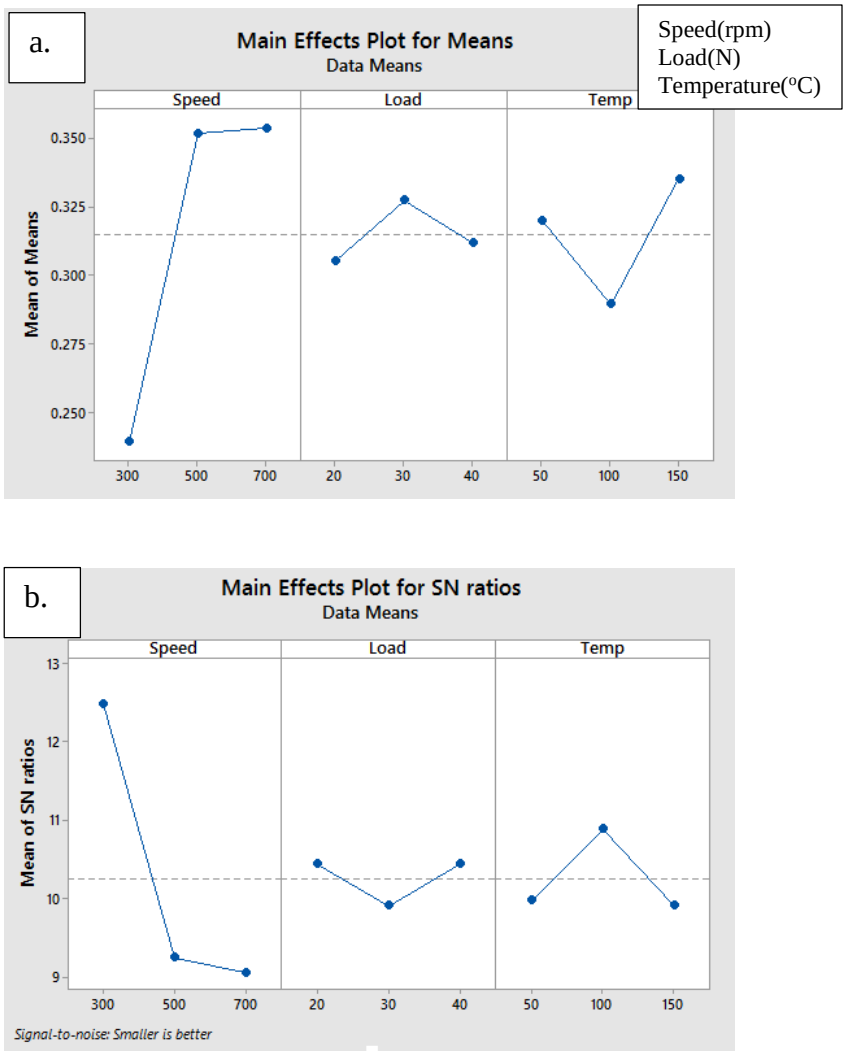

a. Graph between mean of mean and input parameters

b. Graph between mean of SN ratio and input parameters

Figure 31 mean to mean graph of COF

Table 15 COF Response Table for Signal to Noise Ratios of AA6063

Level	Speed	Load	Temp
1	12.487	10.439	9.974

2	9.238	9.903	10.888
3	9.053	10.436	9.916
Delta	3.434	0.536	0.972
Rank	**1**	**3**	**2**

4.3.2.2. Specific Wear rate of AA6063: -

The tribological investigation of POD was done and SWR was calculated for the base material (AA 6063). The SWR increases as the load and the temperature as shown in Figure 32 (a), moreover as the speed increased the SWR increased initially and then decreased as shown in Figure 32 (a). Figure 32 (b) show effect of input parameters on SWR. The response table as shown in Table 16 shows that temperature had maximum impact on the SWR followed by load and speed. The Taguchi analysis shows that the optimum parameter for COF was at a speed of 700rpm, a load of 20N and at 50^{o}C temperature. The FESEM analysis showed that the cliff and edges were present over the wear surface because of micro welding of tribo-pairs. The wear sample also has several voids which were observed during FESEM analysis. The wear debris was scratted above the pin surface. This would increase the SWR.

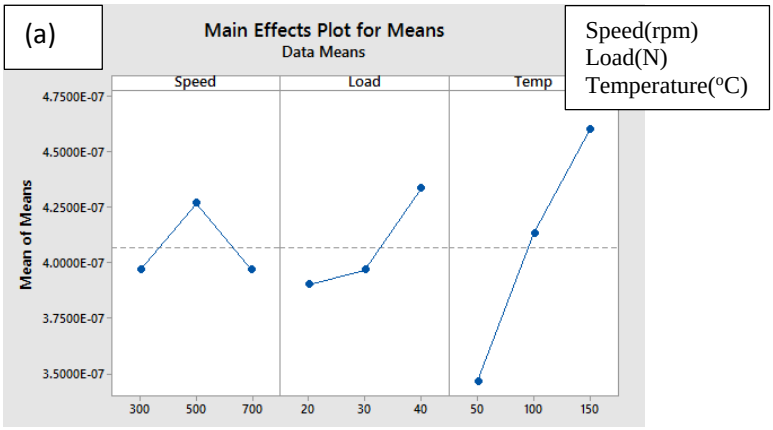

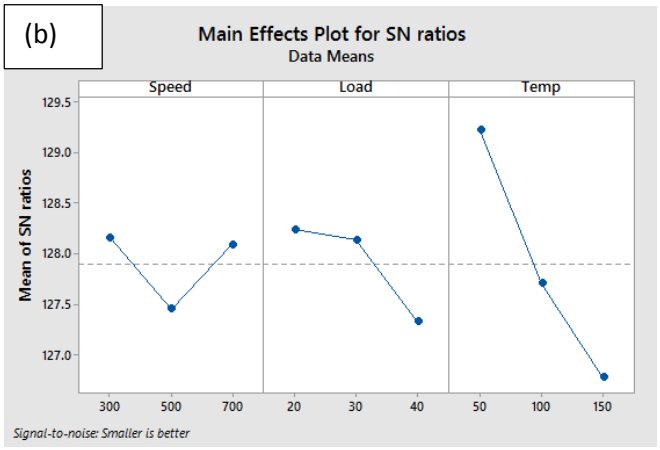

a. Graph between mean of mean and input parameters

b. Graph between mean of SN ratio and input parameters

Figure 32 Effect of parameters on SWR

Table 16 SWR Response Table for Signal to Noise Ratios

Level	Speed	Load	Temp
1	128.2	128.2	129.2
2	127.4	128.1	127.7
3	128.1	127.3	126.8
Delta	0.7	0.9	2.4
Rank	**3**	**2**	**1**

4.3.3. Tribological Analysis of Processed Samples

4.3.3.1. COF of AA6063 composite:

The tribological investigation composite(AA 6063) was done on tribometer according to Taguchi L9 orthogonal array. The variation of COF with respect to FSP process parameters, sliding speed, load and temperature were done as shown in Figure 33 (b) and Figure 34 (a) show effect of input parametes on COF. The increase in temperature decreases the COF up to 100^{o}C but as the temperature was increased up to 150^{o}C the COF increased as shown in Figure 34 (b). The response table as shown in Table 17 shows that type of sample has maximum impact on the COF followed by load and temperature. Sliding

speed had least impact on COF. The Taguchi analysis shows that the optimum parameter for COF were at a speed of 500rpm, load of 60N and at 50^{o}C temperature. Sample 2 had minimum COF values. The decrease in the COF may be due to the stained layer of the marble dust particles [54].

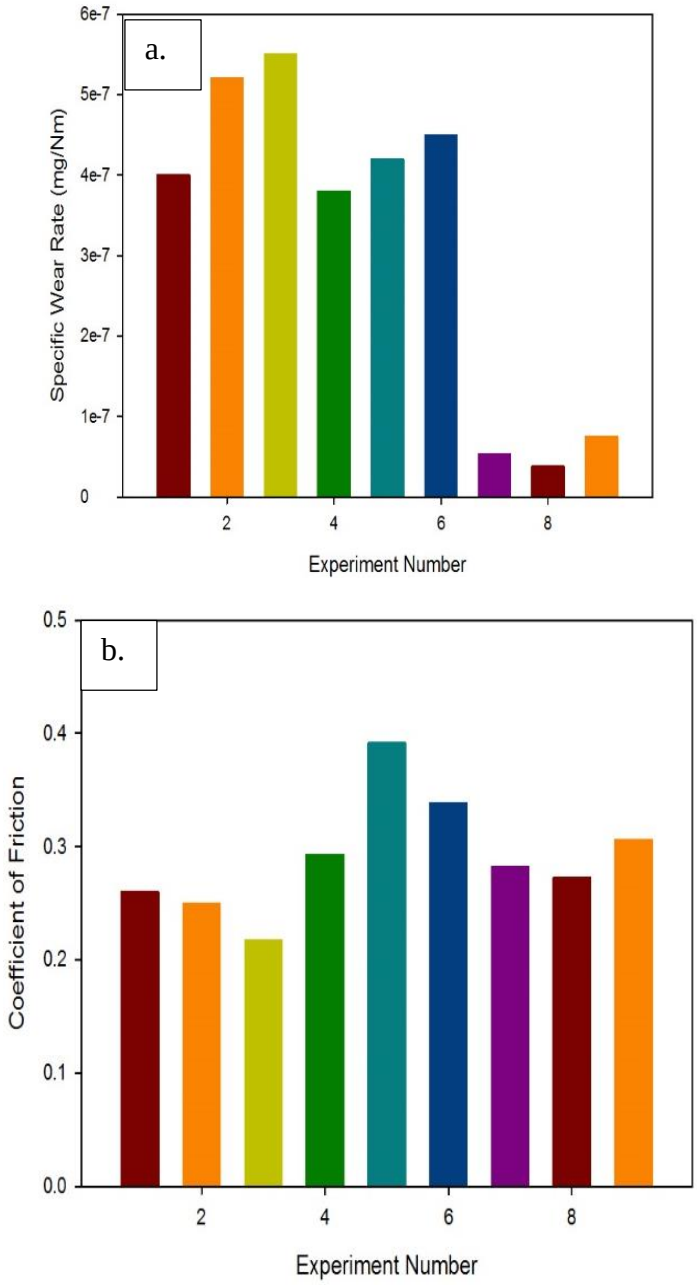

a. Graph between specific wear rate and experiment number of composite

b. Graph between cofficient of friction and experiment number of composite

Figure 33 Processed samples SWR and COF

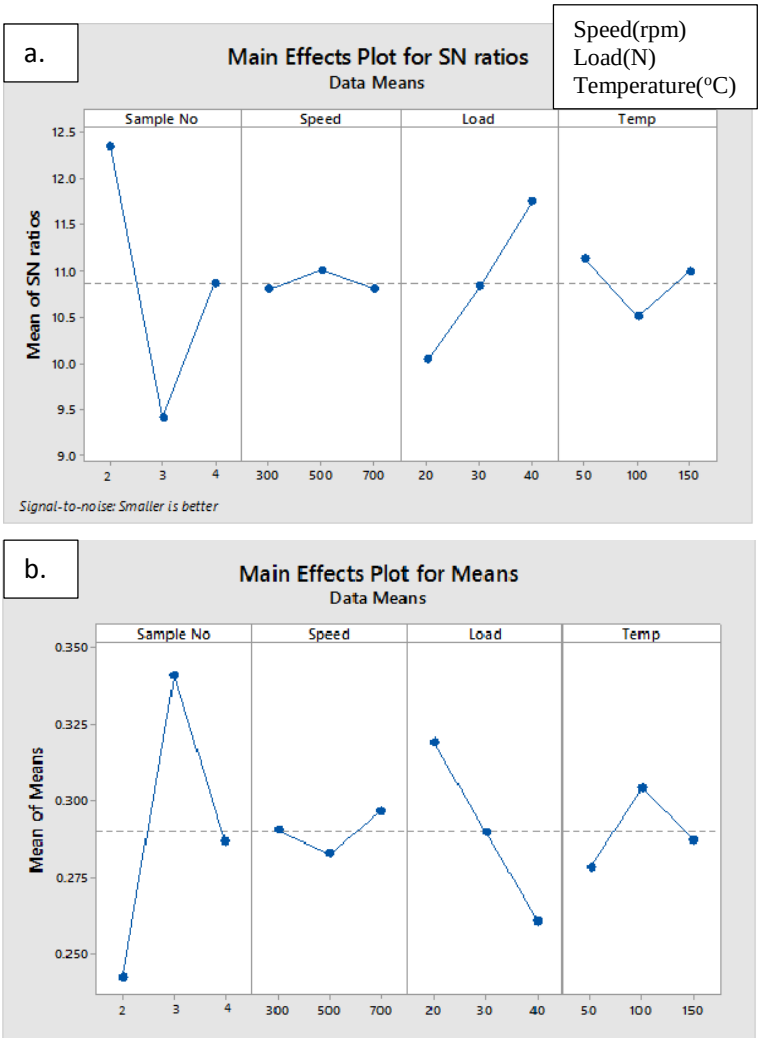

a. Graph between mean of SN ratio and input parameters

b. Graph between mean of mean and input parameters

Figure 34 Mean COF of the processed samples

Table 17 COF Response Table for Signal to Noise Ratios of processed samples

Level	Sample No	Speed	Load	Temp
1	12.342	10.798	10.040	11.124
2	9.407	11.005	10.827	10.501
3	10.861	10.808	11.743	10.984
Delta	2.935	0.207	1.703	0.623
Rank	**1**	**4**	**2**	**3**

4.3.3.2. Effect on Specific Wear Rate of processed samples: -

The tribological investigation composite(AA 6063) was done on tribometer according to Taguchi L9 orthogonal array. The variation of SWR with respect to FSP process parameters, sliding speed, load and temperature was done as shown in Figure 35 (a). The increase in speed, temperature increased the SWR increased as shown in Figure 35 (b). The response table shown in Table 18 shows that type of sample has maximum impact on the SWR followed by temperature and speed. Load had least impact on SWR. The Taguchi analysis shows that the optimum parameter for SWR were at a speed of 300rpm, load of 20N and at 50^{o}C temperature. Sample 4 had minimum SWR values.

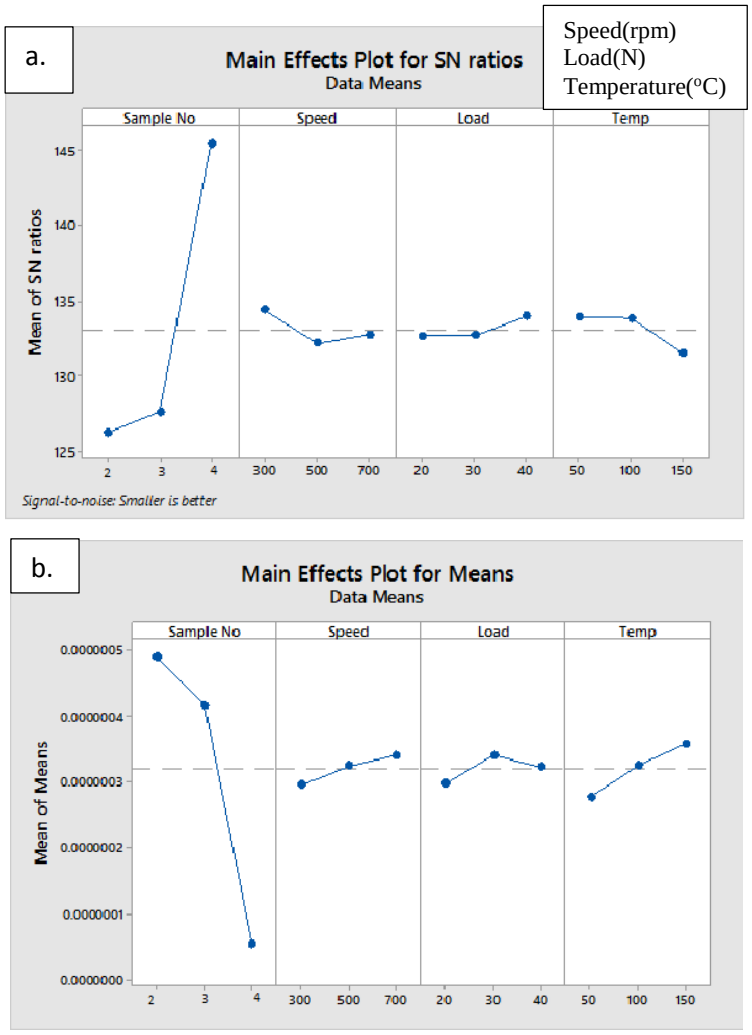

a. Graph between mean of SN ratio and input parameters

b. Graph between mean of mean and input parameters

Figure 35 Graphs of effect process parameters on SWR

Table 18 SWR Response Table for Signal to Noise Ratios of processed samples

Level	Sample No	Speed	Load	Temp
1	126.3	134.4	132.7	134.0
2	127.6	132.2	132.7	133.9
3	145.5	132.7	134.0	131.5
Delta	19.2	2.2	1.3	2.4
Rank	**1**	**3**	**4**	**2**

Field Emission Scanning Electron Microscope analysis of wear tracks

The Microstructure showed smaller grain in F.S.P samples as compared to base material out of which smallest grains were of sample pre-heat temperature at 200^{o}C. the SWR of the processed samples were decreased as compared to the base material. Figure 33 (a) shows the SWR of the processed samples, which shows the improvement in the SWR. The FESEM analysis was carried for the F.S.P samples and it showed that incase of F.S.P at room temperature the voids were smaller and the wear track didn't have cliff edges as in case of base material. Figure 36 is the FESEM image of sample-1, as clearly seen the voids are present over the wear surface. These voids are created due to removal of particle due to impact of shear forces. The cliff edge, debris also present over the surface.

FESEM of the wear track of the samples

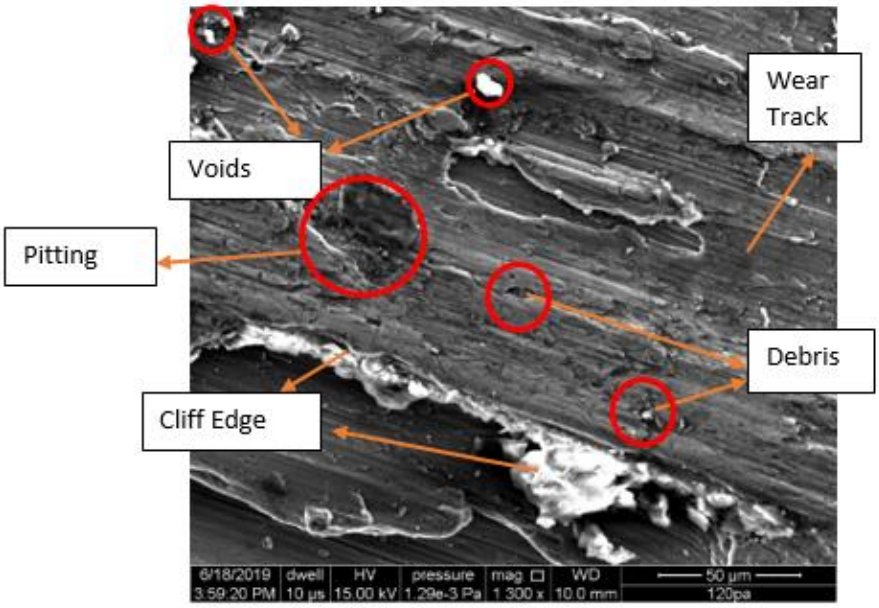

Figure 36 Sample 1

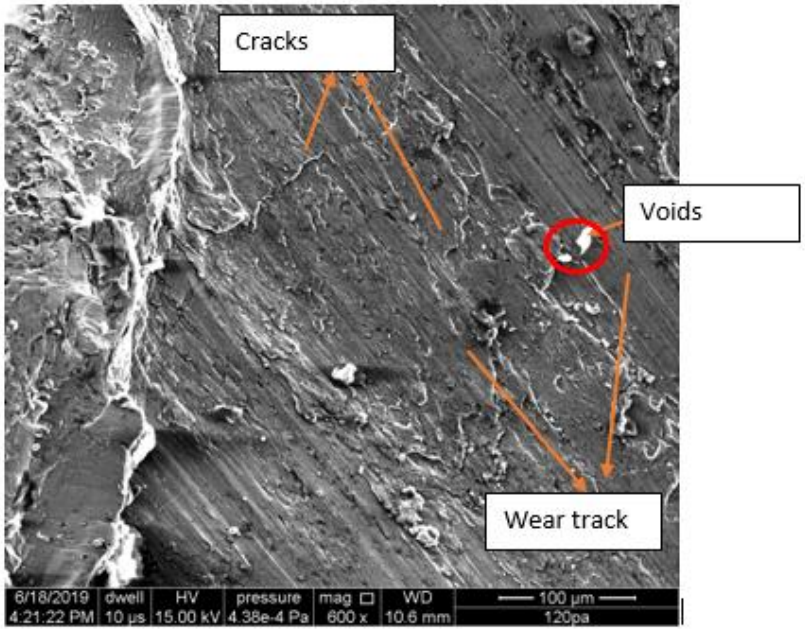

Figure 37 Sample 2

The investigation also shows that the SWR of composite material increases as speed of the disc increase and the temperature increases. But as the load increase up-to 30N it increases but as load further increased upto 40N SWR decreases as shown in Figure 35. According to the analysis of FESEM sample-2 have the voids, cracks on the surface as shown in Figure

37. As in case of sample-3 there were traces of wear debris on the surface but the voids were not observed but the wear track have heat affected cliff edges and the abrasive groove present over the surface.

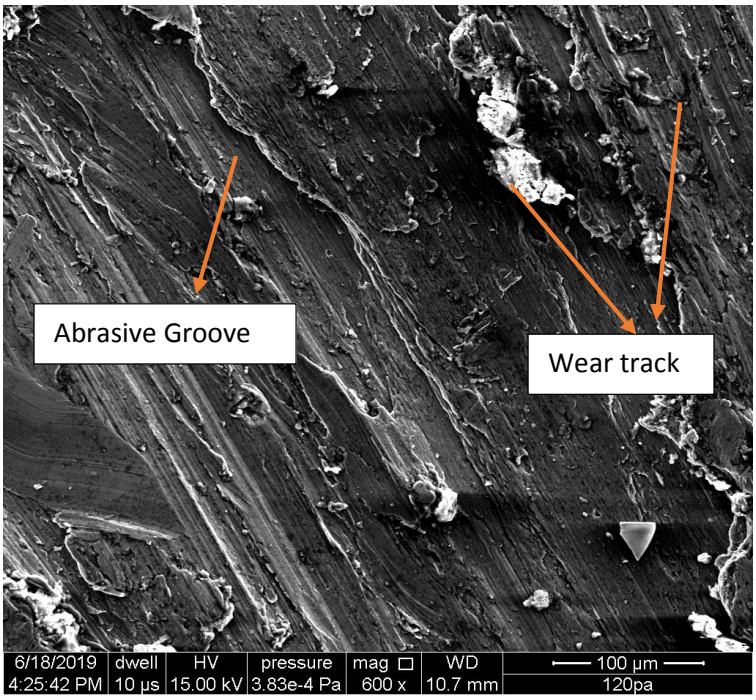

Figure 38 Sample 3

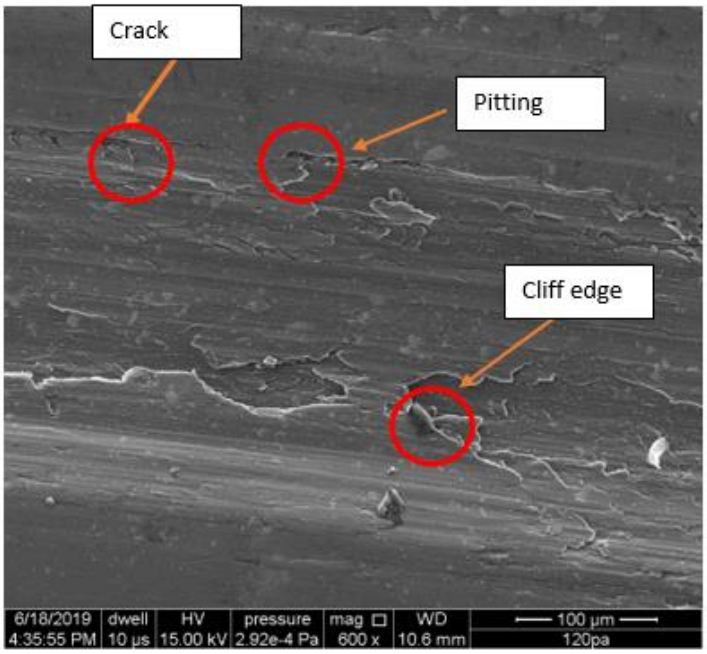

Figure 39 Sample 4

The F.S.P at 200^{o}C pre-heat resulted in compact grain structure which may increase the hardness of the sample. The wear track has micro debris and the micro voids. The effect of the temperature was not much still a micro crack was observed on the surface Figure 39 shows the FESEM image of sample-4 which may be due to the improper bonding of the marble dust and the aluminium alloy. The wear rate may decrease due to the improvement in the grain structure and hardness of the sample.

The FESEM analysis of worn surface was done for determining the defects present over the surface. It was observed that as the defects over the surface decreased as the pre-heat temperature increased. Also it was found that the specific wear rate of composite decreased with the increase in the pre-heat temperature.

Chapter-5

CONCLUSIONS AND FUTURE SCOPE OF STUDY

5.1 Conclusions

The composite of Aluminium alloy with marble dust was fabricated successfully using FSP. The morphological, mechanical and tribological properties of the prepared samples was computed and compared with the base material i.e. AA 6063.

- The micro-hardness for sample-1, sample-2, sample-3, and sample-4 was recorded as 67.29, 57.63, 59.75 and 77.396 Hv respectively.
- The tensile strength for sample-1, sample-2, sample-3, and sample-4 was recorded as 67.29, 97.6, 121 and 202 respectively.
- The morphological analysis revels that the F.S.P samples have finer grain size as compared with base material.
- The XRD results reveal the particles present in the base material AA6063 were Al and Al-Fe-Si. XRD for FSP samples found the presence of Ca, Si, O, Al, and Mg.
- The tribological investigation of Pin on disc was done according to Taguchi L9 orthogonal arrey. Taguchi analysis showed that speed has maximum impact on the Cofficient of friction (COF) followed by temperature and lastely by load.
- The Taguchi analysis showed that temperature had maximum impact on the SWR followed by load and speed. The Taguchi analysis shows that the optimum parameter for COF were at a speed of 700rpm, load of 20N and at 50^{o}C temperature.
- The tribological investigation compisite (AA 6063) was done on tribometer according to Taguchi L9 orthogonal array showed that type of sample has maximum impact on the COF followed by load and temperature. Sliding speed had least impact on COF.
- The Taguchi analysis showed that samples has maximum impact on the Specific wear rate followed by temperature, speed and lastly Load.
- The FESEM revels that the voids, cracks, cliff edges and wear dabris were lesser in case of F.S.P products.

5.2 Future scope of study

- The composite using marble dust can be prepared with different alloys of aluminium as well as other metals.
- The optimization of F.S.P parameters can be done for finer grain size.
- Fabrication of composite can be done with different shape of tool tip.
- The composite can be prepared with other techniques using marble dust as reinforcement.
- The marble dust can be used in different field like it can used as binding agent and replace cement, it can be used in polymer and epoxy to enhance the properties.

REFERENCES

1. Alaneme, K. K, Bodunrin, M. O., & Awe, A. A. (2018). “Microstructure, mechanical and fracture properties of groundnut shell ash and silicon carbide dispersion strengthened aluminium matrix composites”. Journal of King Saud University - Engineering Sciences, 30(1), 96–103
2. Alaneme, K. K, Ekperusi, J.O., & Oke, S. R. (2018). “Corrosion behaviour of thermal cycled aluminium hybrid composites reinforced with rice husk ash and silicon carbide”. Journal of King Saud University - Engineering Sciences, 30(4), 391–397.
3. Govindharajan, B., Manikandan, S., Mohankumar, P., Raghul, R. Ash, R. H. (2015) “Effect of E-waste Aluminium with Fly ash composite for environment safety”, International Journal of Scientific and Research Publications *5*(10), 1–16.
4. Balakrwashnan, M., Dinaharan, I., Palanivel, R., & Sathiskumar, R. (2019). “Influence of friction stir processing on microstructure and tensile behavior of AA6061 / Al 3 Zr cast aluminum matrix composites”. Journal of Manufacturing Processes, 38, 148–157.
5. Balakrwashnan, M, Dinaharan, I, Palanivel, R, & Sathiskumar, R. (2019). “Effect of friction stir processing on microstructure and tensile behavior of AA6061/Al3Fe cast aluminum matrix composites”. Journal of Alloys and Compounds.
6. Bannaravuri, P. K., & Birru, A. K. (2018). “Strengthening of mechanical and tribological properties of Al-4.5%Cu matrix alloy with the addition of bamboo leaf ash”. Results in Physics, 10, 360–373.
7. Bharathi, V, Ramachandra, M., & Srinivas, S. (2017). “Influence of Fly Ash content in Aluminium matrix composite produced by stir-squeeze casting on the scratching abrasion resistance, hardness and density levels”. Materials Today: Proceedings, 4(8), 7397–7405.
8. Chaithanyasai, A, Vakchore, P. R., & Umasankar, V. (2014). “The micro structural and mechanical property study of effects of EGG SHELL particles on the Aluminum 6061”. Procedia Engineering, 97, 961–967.

9. Devaraju. A, Babu. K, & Gnanavelbabu, A (2018). “Investigation on the Mechanical properties of Coconut Bunch fiber Reinforced Epoxy with Al2O3Nano particles Composites for Structural Application”. Materials Today: Proceedings, 5(6), 14252–14257.
10. Dinaharan. I, & Akinlabi. E. T. (2018). “Low cost metal matrix composites based on aluminum, magnesium and copper reinforced with fly ash prepared using friction stir processing”. Composites Communications, 9, 22–26.
11. Dinaharan. I, Balakrwashnan. M., Raja. J. D., & Akinlabi. E. T. (2019). “Microstructural characterization and tensile behavior of friction stir processed AA6061 / Al 2 Cu cast aluminum matrix composites”. Journal of Alloys and Compounds, 781, 270–279.
12. Dinaharan. I, Kalawaselvan. K., & Murugan. N. (2017). “Influence of rice husk ash particles on microstructure and tensile behavior of AA6061 aluminum matrix composites produced using friction stir processing”. Composites Communications, 3, 42–46.
13. Arulmoni, V.J, Ranganath. M. S., Mishra, R. S., “Effect of Process Parameters on Friction Stir Processed Copper and Enhancement of Mechanical Properties of the Composite Material”.
14. Arulmoni, V.J, Ranganath, M. S., Mishra, R. S., “Effect of Single and Multiple-Pass Friction Stir Processing on Microstructure, Hardness and Tensile Properties of a 99.99% Cu with Carbon Nano Tubes”.
15. Gladston, J. A. K., Dinaharan, I., Sheriff, N. M., & Selvam, J. D. R. (2017). “Dry sliding wear behavior of AA6061 aluminum alloy composites reinforced rice husk ash particulates produced using compocasting”. Journal of Asian Ceramic Societies, 5(2), 127–135.
16. Hima, G, C., Prasad D, Ramji K. G., & Vinay, P. V. (2018). “Mechanical Characterization of Aluminium Metal Matrix Composite Reinforced with Aloe vera powder”. Materials Today: Proceedings, 5(2), 3289–3297.
17. Khan, I. M, Megeri R. A., S., & Sadik, S. (2016). “Study of hardness and tensile strength of Aluminium-7075 percentage varying reinforced with graphite and bagasse-ash composites”. Resource-Efficient Technologies, 2(2), 81–88.

18. Jin, Y., Wang, K., Wang, W., Peng, P., Zhou, S., & Huang, L. (2019). “Materials Characterization Microstructure and mechanical properties of AE42 were earth-containing magnesium alloy prepared by friction stir processing”. Materials Characterization, 150, 52–61.
19. Khan, M. M., & Dixit, G. (2017). “Comparative Study on Erosive Wear Response of SiC Reinforced and Fly Ash Reinforced Aluminium Based Metal Matrix Composite”. Materials Today: Proceedings, 4(9), 10093–10098.
20. Mehta, K. M., & Badheka, V. J. (2019). “Wear behavior of boron-carbide reinforced aluminum S.C fabricated by Friction Stir Processing”. Wear, 426–427(December 2018), 975–980.
21. Nagaraj, N., Mahendra, K. V., & Nagaral, M. (2018). “Microstructure and Evaluation of Mechanical Properties of Al-7Si-Fly Ash Composites”. Materials Today: Proceedings, 5(1), 3109–3116.
22. Patel, S., Rana, R. S., & Singh, S. K. (2017). “Study on mechanical properties of environment friendly Aluminium E-waste Composite with Fly ash and E-glass fiber” Materials Today: Proceedings, 4(2), 3441–3450.
23. Prabhu, M. S., Perumal, A. E., Arulvel, S., & Wassac, R. F. (2019). “Friction and Wear Measurements of Friction Stir Processed Aluminium Alloy 6082/CaCO3 Composite” Measurement S0263-2241(19)30379-3.
24. Reddy, B. R., & Srinivas, C. (2018). “Fabrication and Characterization of Silicon Carbide and Fly Ash Reinforced Aluminium Metal Matrix Hybrid Composites” Materials Today: Proceedings, 5(2), 8374–8381.
25. Kumar, S, Shalini, T, Kumar S., K. K., Thavamani, R., & Subramanian, R. (2018). “Bagasse Ash Reinforced A356 Alloy Composite: Syntheswas and Characterization” Materials Today: Proceedings, 5(2), 7123–7130.
26. Shamim, S., Singh, H., Sasikumar, C., & Yadav, D. K. (2017) “Microstructures and Mechanical Properties of Al-Si-Mg-Ti/Egg Shell Particulate Composites” Materials Today: Proceedings, 4(2), 2887–2892.
27. Tang, J., Shen, Y., & Li, J. (2019). “Influences of friction stir processing parameters on microstructure and mechanical properties of SiC / Al composites fabricated by multi-pin tool” Journal of Manufacturing Processes, 38, 279–289.

28. Tiwari, S. K., Soni, S., Rana, R. S., & Singh, A. (2017). “Effect of Heat Treatment on Mechanical Properties of Aluminium Alloy-Fly ash Metal Matrix Composite” Materials Today: Proceedings, 4(2), 3458–3465
29. Vipin, Yuvraj N. (2016). “Wear Characteristics of Al5083 Surface Hybrid Nano-composites by Friction Stir Processing” Transactions of the Indian Institute of Metals, Transactions of the Indian Institute of Metals, 1111-1129.
30. Yuvaraj, N., & Aravindan, S. (2015). “Fabrication of Al5083 / B 4 C surface composite by friction stir processing and its tribological characterization” Integrative Medicine Research, 4(4), 398–410.
31. Zhao, H., Pan, Q., Qin, Q., Wu, Y., & Su, X. (2019). “A Effect of the processing parameters of friction stir processing on the microstructure and mechanical properties of 6063 aluminum alloy”. Materials Science & Engineering A, 751, 70–79.
32. Loureiro, A., & Rodrigues, D. (2012). “Influence of Process Parameters on the Mechanical Enhancement of Copper- DHP by FSP”, Advanced Materials Research Vol. 445 pp 631-636.
33. Arulmoni, V. J., & Mishra, R. S. (2014). “Friction Stir Processing of Aluminum alloys for Defense Applications”, International Journal of Advance Research and Innovation Volume 2, Wassue 2, 337-341.
34. Cartigueyen, S., & Mahadevan, K. (2015). “Role of Friction Stir Processing on Copper and Copper based Particle Reinforced Composites – A Review”, *2*(2), 133–145.
35. Dinaharan, I., Kalawaselvan, K., Akinlabi, E. T., & Davim, J. P. (2017). “Microstructure and wear characterization of rice husk ash reinforced copper matrix composites prepared using friction stir processing, SC. Journal of Alloys and Compounds”.
36. Cavaliere, P., "Mechanical properties of Friction Stir Processed 2618/Al2O3 metal matrixcomposite," Composites Part A: Applied Science and Manufacturing, vol. 36, pp. 1657-1665, 2005.
37. Karthik, G. M., Ram, G. D. J., & Kottada, R. S. (2016). “A Friction stir selective alloying”. Materials Science & Engineering A, 684, 186–190.

38. Hodder K. J., Izadi H., McDonald A. G., and Gerlich A. P., (2012) "Fabrication of aluminum–alumina metal matrix composites via cold gas dynamic spraying at low pressure followed by friction stir processing," Materials Science and Engineering: A, vol. 556, pp. 114-121.
39. Xue, P., Xiao, B. L., & Ma, Z. Y. (2013). "Achieving Large-were a Bulk Ultra fine Grained Cu via Submerged Multiple-pass Friction Stir Processing", 29(12), 1111–1115.
40. Cobden, R, Alcan, Banbury (1994) "Aluminium: Physical Properties, Characteristics and Alloys" Training in Aluminium Application technologies, lecture 1501.
41. Cartigueyen, S., & Mahadevan, K. (2015). "Role of Friction Stir Processing on Copper and Copper based Particle Reinforced Composites – A Review", 2(2), 133–145.
42. Prillhofer, R., Rank G., J. Berneder, H. Antrekowitsch, P.J. Uggowitzer, S. Pogatscher (2014), "Property criteria for automotive Al-Mg-Si sheet alloys", Materials 7 (7) 5047–5068.
43. Mukhopadhyay, P. (2012), "Alloy designation, processing, and use of AA6XXX series aluminium alloys", Int. Sch. Res. Not. e165082.
44. Ceresara, S., Russo E. D, Fiorini P., Giarda A. (1970), "Effect of Si excess on the ageing behaviour of Al-Mg2Si 0.8% alloy", Mater. Sci. Eng. 5 (4) 220–227.
45. Gupta A.K., Lloyd D.J. (2001), "Precipitation hardening in Al–Mg–Si alloys with and with- out excess Si, Mater". S.A. Court Sci. Eng. A 316 (1–2) 11–17.
46. Poznak, A., Sanders, P. (2016), "The influence of low temperature clustering on strengthening precip- itation in Al-Mg-Si alloys", Light Met. 237–243.
47. Bhattamwashra, A.K., Lal, K. (1997), "Microstructural studies on the effect of Si and Cr on the intergra- nular corrosion in Al-Mg-Si alloys", Mater. Des. 18 (1) 25–28.
48. Liang W.J., Rometsch P.A., Cao L.F., Birbilwas N. (2013), "General aspects related to the corrosion of 6xxx series aluminium alloys: exploring the influence of Mg/Si ratio and Cu", Corros. Sci. 76 119–128.

49. Lakshmi, K. Subbaiah,J. Sarojini and Shabana (2017), "Study of Mechanical properties and Wear behaviour of Sugarcane ash reinforced Aluminium composite", International Journal of Mechanical Engineering and Technology, vol. 8, no. 6, pp. 597606.
50. Prasat, V., Subramanian, R., N. Radhika, and Anandavel B. (2011), "Dry sliding wear and friction studies on AlSi10Mg fly ash graphite hybrid metal matrix composites using Taguchi method", Tribology, vol. 5, no. 2, pp. 211.
51. Atuanya,U., Ibhadode, A. O. A., and Dagwa, I. M. (2012), "Effects of breadfruit seed hull ash on the microstructure and properties of Al-SiFe alloy/breadfruit seed hull ash particulate composites", Results Phys., vol. 2, pp. 142149.
52. Apasi, D. S. Yawas, S. Abdulkwereem, and M. Y. Kolawole (2016), "Improving Mechanical Properties of Aluminium alloy through addition of Coconut Shell-ash", Journal of Science and Technology, vol. 36, no. 3, pp. 3443.
53. Hassan, B. and Aigbodion, V. S. (2015), "Effects of eggshell on the microstructures and properties of Al Cu Mg/eggshell particulate composites", J. King Saud Univ. - Eng. Sci., vol. 27, no. 1, pp. 4956.
54. Sharma, V.K, Singh, R.C and Chaudhary, R (2018), "Wear and friction behaviour of aluminium metal composite reinforced with graphite particles", Int. J. Surface Science and Engineering, Vol. 12, Nos. 5/6, 419–432.
55. Sharma, V. K., Singh, R. C., & Chaudhary, R. (2017). "Effect of flyash particles with aluminium melt on the wear of aluminium metal matrix composites" Engineering Science and Technology, an International Journal Effect of flyash particles with aluminium melt on the wear of aluminium metal matrix composites. Engineering Science and Technology, an International Journal, 20(4), 1318–1323.